ECMWF COPERNICUS REPORT

Copernicus Climate Change Service

Algorithm Theoretical Basis Document

Ocean Colour Version 6.0

Issued by: PML Applications / Thomas Jackson

Date: 17/11/2022

Ref: WP2-FDDP-2022-04_C3S2-Lot3_ATBD-of-v6.0-OceanColour-product_v1.1

Official reference number service contract: 2021/C3S2_312a_Lot3_METNorway/SC1

PROGRAMME OF THE EUROPEAN UNION

IMPLEMENTED BY ECMWF

Please cite this data product as: Jackson et al. (2022) *Ocean colour daily data from 1997 to present derived from satellite observations, Version 6.0*. Copernicus Climate Change Service (C3S) Data Store (CDS), accessed <DD Month YYYY>, https://doi.org/10.24381/cds.f85b319d.

A suggested citation for this document is: Jackson, T., Hockley, K., Calton, B., Chuprin, A. (2022) *C3S Ocean Colour Version 6.0: Algorithm Theoretical Basis Document*. Issue 1.1. E.U. Copernicus Climate Change Service. Document ref. WP2-FDDP-2022-04_C3S2-Lot3_ATBD-of-v6.0-OceanColour-product.

Contributors

PML APPLICATIONS
Thomas Jackson
Kim Hockley
Ben Calton
Andrei Chuprin

History of modifications

Version	Date	Description of modification	Chapters / Sections
1.0	31/01/2022	Creation. *Jackson et al.* (2020) C3S Ocean Colour Version 5.0: Algorithm Theoretical Basis Document, issue 1.1. E.U. Copernicus Climate Change Service, document ref. D1.OC.2-v5.0_ATBD_of_v5.0_Ocean_Colour_products_v1.1 was used a basis for this document.	All
1.1	17/11/2022	Document revised to account for feedback from independent review, and published.	All

List of datasets covered by this document

This document refers to CDR 6.0 and the corresponding temporal extensions (ICDR). For an outline of the version development leading to version 6.0, see the relevant section in this document.

Deliverable ID	Product title	Product type (CDR, ICDR)	Version number	Delivery date
WP2-FDDP-2022-04_C3S2-Lot3_DatasetDelivery-of-v6.0-OC-CDR_v1.0	Ocean Colour ECVs	CDR	6.0	15 June 2022
WP2-ICDR-OC-v6.0_C3S2-Lot3_DatasetDelivery-of-v6.0-OC-ICDR_v1.0	Ocean Colour ECVs	ICDR	6.0	27 July 2022
WP2-ICDR-OC-v6.0_C3S2-Lot3_DatasetDelivery-of-v6.0-OC-ICDR_v1.0	Ocean Colour ECVs	ICDR	6.0	31 October 2022
WP2-ICDR-OC-v6.0_C3S2-Lot3_DatasetDelivery-of-v6.0-OC-ICDR_v1.0	Ocean Colour ECVs	ICDR	6.0	31 January 2022

Related documents

Reference ID	Document
C3S2_SQAD	Jackson, T. (2023) *C3S Ocean Colour Version 6.0: System Quality Assurance Document*. Issue 1.1. E.U. Copernicus Climate Change Service. Document ref. WP3-SQAD-OC-v6.0_C3S2-Lot3_SQAD-of-v6.0-OceanColor-product.
C3S2_PQAD	Jackson, T., et al. (2023) *C3S Ocean Colour Version 6.0: Product Quality Assurance Document*. Issue 1.1. E.U. Copernicus Climate Change Service. Document ref. WP1-PDDP-OC-v6.0_C3S2-Lot3_PQAD-of-v6.0-OceanColour-product.
C3S2_PQAR	Jackson, T., Calton, B., Hockley, K. (2023) *C3S Ocean Colour Version 6.0: Product Quality Assessment Report*. E.U. Copernicus Climate Change Service. Document ref. WP2-FDDP-2022-04_C3S2-Lot3_ PQAR-of-v6.0-OceanColour-product.
C3S2_PUGS	Jackson, T., Calton, B., Hockley, K. (2023) *C3S Ocean Colour Version 6.0: Product User Guide and Specification*. Issue 1.1. E.U. Copernicus Climate Change Service. Document ref. WP2-FDDP-2022-04_C3S2-Lot3_ PUGS-of-v6.0-OceanColour-product.
OC_CCI-SSD	OC_CCI System Specification Document. Available at https://climate.esa.int/en/projects/ocean-colour/key-documents/ [last accessed 17th November 2022].
OC_CCI-ATBD	OC_CCI Algorithm Theoretical Baseline Document. Available at https://climate.esa.int/en/projects/ocean-colour/key-documents/ [last accessed 17th November 2022].
OC_CCI-PUG	OC_CCI Product User Guide. Available at https://climate.esa.int/en/projects/ocean-colour/key-documents/ [last accessed 17th November 2022].
OC_CCI-IODD	OC_CCI Input Output Definition Document, D2.8 1.1 [PDF]
OC_CCI-ATBD-DBCM	OC_CCI ATBD Ocean Colour Data Bias Correction and Merging. Available at https://climate.esa.int/en/projects/ocean-colour/key-documents/ [last accessed 17th November 2022].
POLYMER ATBD	ATBD Polymer atmospheric correction algorithm. Available at https://climate.esa.int/en/projects/ocean-colour/key-documents/ [last accessed 17th November 2022].

Acronyms

Acronym	Definition
ACRR	Atmospheric correction round robin
AC	Atmospheric Correction
AOP	Apparent Optical Property
AVHRR	Advanced Very-High-Resolution Radiometer
BEAM	Basic ENVISAT Toolbox for (A)ATSR and MERIS
C2Rcc	Case 2 Regional CoastColour
C3S	Copernicus Climate Change Service
CBQ	Common Best Quality
CCD	Charge-coupled device
CF	Climate and Forecast (a community of climate and forecast data producers that have agreed metadata standards).
Chl (also Chl-a)	Chlorophyll (Chlorophyll-a)
CZCS	Coastal Zone Color Scanner
ECV	Essential Climate Variable
EO	Earth Observation
ERA-5	ECMWF Reanalysis 5th Generation
ESA	European Space Agency
fqMorel	A correction for surface reflectance where f is a dimensionless coefficient relating the irradiance reflectance to IOPs and Q is the bidirectional function.
GAC	Global Area Coverage
GCOS	Global Climate Observing System
HPLC	High Performance Liquid Chromatography
IBQ	Individual Best Quality
IdePIX	Identification of Pixels (neural network for pixel identification)
IOPs	Inherent Optical Properties
IWRR	In water round robin
L2gen	NASA level2 data generation (part of SeaDAS)
L3bin	The level 3 product binning program contained within SeaDAS
LAC	Local Area Coverage
LUT	Look Up Table
MEGS	MERIS Ground Segment
MERIS	Medium Resolution Imaging Spectrometer
MLAC	Merged LAC
MODIS	NASA Moderate Resolution Imaging Spectroradiometer
NASA	National Aeronautics and Space Administration
NaN	Not a number (this is a null value used in data processing)
NCEP	National Centers for Environmental Prediction (NCEP)/National Center for Atmospheric research (NCAR) Reanalysis dataset

NOAA	National Oceanic and Atmospheric Administration
NOMAD	NASA bio-Optical Marine Algorithm Dataset
NWP	Numerical weather prediction
OBPG	Ocean Biology Processing Group
OC	Ocean Colour
OCx	The OC2, OC3, OC4, OC5, and OC6 are all NASA Ocean Colour algorithms for estimating chlorophyll-a. The Ocx algorithm switches across more than one of these.
OC-CCI	Ocean Colour Climate Change Initiative
OCI	Ocean Colour Index
OCL	Offset Control Loop
OLCI	Ocean and Land Colour Instrument
PML	Plymouth Marine Laboratory
POLYMER	POLYnomial based algorithm applied to MERIS: algorithm aimed at recovering the radiance scattered and absorbed by the oceanic waters (also called Ocean Colour) from the signal measured by satellite sensors in the visible spectrum.
QAA	Quasi-Analytical Algorithm
R2018	The 2018 Mass Reprocessing of level1 and level2 data by NASA
RMSE	Root-mean-square error
RR	Round Robin
R_{rs}	Remote Sensing Reflectance
SeaDAS	SeaWiFS Data Analysis System
SeaWIFS	Sea-viewing Wide Field of view Sensor
SNAP	Sentinels Application Platform
SNR	Signal to Noise Ratio
VIIRS	Visible Infrared Imaging Radiometer Suite

General definitions

Atmospheric Correction

Atmospheric correction is the process of removing the effects of the atmosphere on the satellite images so that we can obtain information about the surface of the Earth. Atmospheric effects in optical remote sensing are significant and complex but can be largely considered as absorbing or scattering factors. Also keep in mind that the light reaching the satellite borne sensor has passed through the atmosphere twice, from the sun to the surface and then back to the sensor. For ocean colour remote remote sensing, the surface signal from the ocean is typically ≤10% of the total signal received by the satellite (with the other 90+% coming from the atmosphere.

Binning

In the context of this document, binning refers to the process of aggregating data into bins. This is an essential process when it comes to merging data from multiple sensors. Each remote

sensing platform used to observe the Earth collects data in a manner that is constrained by the sensor design and satellite orbit. This means that different sensors will collect data at difference spatial resolutions and viewing geometries. Once the data has been processed at its native resolution it can be binned onto a defined grid for easier use.

Chlorophyll-a
Chlorophyll-a is a green pigment and the most prevalent photosynthetic pigment in both terrestrial and marine photosynthetic organisms. As an indicator of phytoplankton abundance, and therefore the base of the marine foodweb, chlorophyll-a concentration (chl-a) is recognised as an Essential Climate Variable. Oceanic chlorophyll-a is usually measured in units of mg m^{-3}, with concentrations ranging over multiple orders of magnitude.

Climate Data Record
The term Climate Data Record has a specific definition developed by the CEOS-CGMS Joint Working Group on Climate in 2020. The CEOS definition scheme defines three types of climate data records: 1) Fundamental Climate Data Records (FCDRs) consist of a consistently processed time series of uncertainty-quantified sensor observations calibrated to physical units, located in time and space, and of sufficient length and quality to be useful for climate science or applications; 2) Climate Data Records (CDRs) consist of a consistently processed time series of uncertainty-quantified retrieved values of a geophysical variable or related indicator, located in time and space, and of sufficient length and quality to be useful for climate science or applications; 3) Interim Climate Data Records (ICDRs) are consistently processed times series of uncertainty-quantified estimates of CDR values produced with better timeliness than, but otherwise minimising differences with, the estimated CDR values.

Essential Climate Variable
An Essential Climate variable (ECV) is a physical, chemical, or biological variable or a group of linked variables that critically contributes to the characterisation of Earth' s climate. The Global Observing Systems Information Center (GOSIC) provides further background, definitions, requirements, network information, and data sources for the ECVs.

In-water algorithms
The term 'in-water' is used to describe algorithms that estimate in-water properties of the surface water from the surface reflectance signal. These algorithms often provide estimates of concentrations of substance (such as chlorophyll-a or sediment) but could also provide estimates of Inherent Optical Properties IOPs such as absorption or scattering.

Level-[x] remote sensing data
Within remote sensing and ocean colour applications, datasets are often described in terms of levels. The level is representative of the amount of processing that has been performed. Level-0 is the rawest data format available. It is full resolution data, as it comes from the instrument, with some processing applied to remove artefacts from data communication between the satellite and the ground stations. Level-1 data is full resolution sensor data with time-

referencing, ancillary information, including radiometric and geometric calibration coefficients and georeferencing parameters, computed and added to the file. Level-2 refers to derived geophysical variables (such as water-leaving reflectance or ocean colour products) at full resolution. This will have required processing to remove the atmospheric component of the signal. Pixels will also be masked by use of data quality flags. Level-3 data is a binned version of the level-2 products at a given temporal and spatial resolution.

Masking

Masking is the process of setting pixels to NaN or blank values where a flag has been raised that the data would not be of sufficient quality for the intended purpose (or processing has failed). There are many factors that can lead to remote sensing data being of insufficient quality for a climate data record, so we shall not list them all here, but commonly applied masks in ocean colour remote sensing include cloud, cloud shadow, land, glint, and algorithm failure masks.

Match-ups

In the context of this document a match-up refers to a matched pair of in situ and remote sensing data. These measurements are matched based on their time and location information where some permitted time or space offset is permitted, for example we might match an in situ measurement to the closest pixel on the satellite data grid for the same day of observation. It is also of note that these measurements are also made using information at very different scales; an in situ measurement of chlorophyll-a might be from a litre of filtered seawater while the remote sensing estimate may be derived over a pixel 1km square (or larger).

Phytoplankton

Phytoplankton are aquatic microscopic photosynthetic organisms. This group includes some bacteria, protists, and single-celled plants. There is a great diversity in appearance and function across phytoplankton, with orders of magnitude in size between the largest and smallest phytoplankton. Given their photosynthetic abilities, phytoplankton form the base of the marine food web. Phytoplankton growth primarily depends on the availability of sunlight and nutrients.

Remote sensing reflectance

Remote Sensing Reflectance, $R_{rs}(\lambda)$, has units of sr^{-1} (per steradian) and is the water-leaving radiance, corrected for bidirectional effects of the air-sea interface and sub-surface light field, normalised by downwelling solar irradiance, Ed(λ), just above the sea surface. This is usually measured at multiple wavelengths by a given ocean colour sensor, so R_{rs} is a spectral product. R_{rs} is the primary variable of the Ocean Colour ECV, and the chlorophyll-a products are derived from the Rrs data.

Table of Contents

Scope of the document

This document is the Algorithm Theoretical Basis Document (ATBD) for the Ocean Colour ECV processing system and covers both the remote-sensing reflectance (R_{rs}) and chlorophyll-a products. The processing chain is built and run by the Plymouth Marine Laboratory (PML), and at the time of writing, ingests data from the Sea-viewing Wide Field of view Sensor (SeaWIFS), NASA Moderate Resolution Imaging Spectroradiometer (MODIS), Medium Resolution Imaging Spectrometer (MERIS), Visible Infrared Imaging Radiometer Suite (VIIRS) and Ocean and Land Colour Instrument (OLCI) instruments. This document describes the techniques and algorithms used for the merged sensor products (and the methods for choosing those algorithms) in a manner that accounts for inter-sensor differences and optimises product quality.

Executive summary

The Ocean Colour Essential Climate Variable includes **daily** measurements of the **oceanic surface water reflectance** and **chlorophyll-a concentration**. These data can be used to study the distribution of **phytoplankton and other optically active materials** (such as coloured dissolved material, sediments, and other particles). These data are therefore **essential** to global studies of **the ocean biosphere**.

This document describes the **algorithm** and **processing** which underpins the **Version 6.0 C3S Chlorophyll-a and remote-sensing reflectance (R_{rs})** data record products available through the Copernicus Climate Change Service (Ocean Colour).

The process of generating ocean colour data from multiple sensors is a **multi-stage process** that has to ensure that data are **corrected for atmospheric effects**, **harmonised** to account for sensor differences, processed in **a consistent manner**, **masked** to remove poor quality data, binned onto a **common data grid**, and makes use of the **state of the art algorithms**.

Recent improvements between the V5.0 and the V6.0 datasets include:

- Inclusion of the MERIS-4th reprocessing. V5.0 used the MERIS 3rd reprocessing.
- Addition of data from the Ocean and Land Colour Instrument (OLCI) aboard Sentinel 3B.
- We have upgraded the Quasi-Analytical algorithm (QAA) used in the band shifting to QAAv6 (the V5.0 data used the QAAv5).
- Minor update to the inter-sensor bias correction.
- MODIS and VIIRS data have been dropped from the record after 2019 due to concerns about the continued quality of data from the ageing sensors.
- Temporal extension of the dataset into 2022.

When using these products there are a few **things to note**:

1. All input sensors are passive, making use of the sun as the illumination source for observation, so data coverage exhibits a strong seasonal signal at high latitudes.

2. Many Ocean Colour variables, such as chlorophyll-a, exhibit a log-normal distribution at the global scale. This means that when you perform statistical analyses, such as calculating mean values or standard deviations, it is often more appropriate to log-transform the values prior to analysis in order to maintain the required underlying statistical assumptions.
3. Great care is taken to create a harmonised record across multiple ocean colour sensors and we perform analysis to ensure that post inter-sensor-bias-correction sensor records are aligned. However, because different combinations of sensors and atmospheric correction schemes have differing capabilities to observe optically complex conditions, we see changes in the coverage of the record at the large scale as sensors add to or drop from the record. For example, there are more coastal observations when MERIS is contributing to the record.

1. Instruments

Details on the instruments contributing to the V6.0 Ocean Colour record are given below and summarised in Table 1.

1.1 MODIS Aqua

The NASA Moderate Resolution Imaging Spectroradiometer (MODIS) is carried on both the Terra and Aqua platforms. Only Aqua-MODIS is being considered in this project due to residual issues with Terra-MODIS, though NASA's Ocean Biology Processing Group (OBPG) are working to resolve these as far as possible. Where MODIS is mentioned herein it refers to purely Aqua-MODIS. Aqua-MODIS has been available since 2002 and is still active at the time of writing. Due to concerns about the quality of the data from the aging MODIS aqua Sensor we have not included MODIS data after the end of 2019. MODIS aqua is maintained in a sun synchronous orbit with observations made on the ascending pass with an equator crossing time of 13:30. Further information can be found at modis.gsfc.nasa.gov/about/ (accessed October 2022).

1.2 SeaWiFS

The Sea-viewing Wide Field-of-view Sensor (SeaWiFS) is carried on the Orbview-2 (a.k.a. Sea Star) spacecraft and was operational for approximately 12.5 years, with occasional periods of outage from 2008 onwards. The mission ended in 2010 when the spacecraft developed faults that could not be rectified. During its operation the satellite maintained a sun synchronous orbit with observations made on the descending path with equator crossing time of Noon+20 mins. Further details can be found at oceancolor.gsfc.nasa.gov/SeaWiFS/SEASTAR/SPACECRAFT.html (accessed October 2022).

1.3 MERIS

The ESA Medium Resolution Imaging Spectrometer (MERIS) was launched on board the Envisat satellite in 2002. The MERIS instrument is composed of five individual sensors (cameras) that together cover the complete swath width. The mission ended abruptly in April 2012 due to an unknown failure and loss of communication. It had two spatial modes: full resolution (~300 m) and reduced resolution (~1.2 km at nadir). MERIS was 13arameteri in a sun synchronous orbit with observations made on the descending path with mean local solar time (MLST) of 10:00. Further information can be found at earth.esa.int/eogateway/instruments/meris/description (accessed October 2022).

1.4 VIIRS

Hosted on board the SUOMI satellite, the Visible Infrared Imaging Radiometer Suite (VIIRS) was launched in October 2011 and was designed as a successor to the MODIS instruments combined with some Advanced Very-High-Resolution Radiometer (AVHRR) capabilities. There were initial concerns that this may have compromised the quality compared to MODIS, but ongoing calibration efforts by NASA's OBPG have radically improved the products over the open ocean (case 1). The band set may still restrict its utility for case 2 waters (where the optical properties are not correlated with chlorophyll-a concentration).

1.5 OLCI

The OLCI (Ocean and Land Colour Instrument) is a medium-resolution imaging spectrometer that, like MERIS, uses five cameras to provide a wide field of view. OLCI improves upon MERIS with features such as six additional spectral bands, higher-end signal to noise ratio (SNR), and reduced solar glaring. There are now two OLCI sensors in operation, OLCI 3A (aboard the Sentinel-3A satellite) and OLCI 3B (aboard the Sentinel-3B satellite). We use data from both of these sensors in the v6.0 data production.

Table 1: Details of the Ocean Colour Instruments contributing to the dataset.

SENSOR / DATA SOURCE	AGENCY	SATELLITE	OPERATING DATES	SWATH (KM)	SPATIAL RESOLUTION (M)	# OF BANDS	SPECTRAL COVERAGE (NM)
MERIS	ESA (Europe)	ENVISAT	01/03/02 – 09/05/12	1150	300/1200	15	412-1050
SeaWiFS	NASA (USA)	OrbView-2	01/08/97 – 14/02/11	2806	1100	8	402-885
MODIS	NASA (USA)	Aqua	04/05/2002-present	2300	250/500/1000	36	405-14,385
OLCI 3A	ESA (Europe)	Sentinel 3A	16/02/2016 – present	1270	300/1200	21	400 – 1020
OLCI 3B	ESA (Europe)	Sentinel 3B	25/04/2018 – present	1270	300/1200	21	400 – 1020
VIIRS	NOAA (USA)	Suomi NPP	28/10/2011 – present	3000	375/750	22	402 – 11,800

2. Input and auxiliary data

2.1 MODIS

The MODIS data used as input to the ocean colour CDR processing chain were :

- The 1-km resolution level 1A data complete global set (2002 – end of 2019, the latest reliable date) from the R2018 reprocessing release.
- Supporting ancillary data (attitude and ephemeris) to allow geolocation and processing to level 1B and higher.

In order to apply many of the later sensor corrections, POLYMER and other algorithms now require access to the "level 1C" dataset, which is essentially the result of running SeaDAS l2gen up to the point of, but not including, atmospheric correction. The R2018 MODIS L1A dataset has therefore been processed to L1C for all granules available.

MODIS Level 1 data can be found at:
oceandata.sci.gsfc.nasa.gov/directdataaccess/Level-1A/Aqua-MODIS (accessed October 2022)
MODIS Geo location data can be found at:
oceandata.sci.gsfc.nasa.gov/directdataaccess/Geo-Location/Aqua-MODIS (accessed October 2022)

2.2 SeaWiFS

The SeaWiFS data used as input to the Ocean Colour CDR were:

- The 4-km GAC and, where available, 1-km MLAC level 1a complete global set (1997-2010) R2018.0.
- The 4-km GAC and, where available, 1-km MLAC level 2 complete global set (1997-2010) R2018.0.

Both level 1 and level 2 data are required as: 1) L2gen was deemed the most appropriate processor for SeaWiFS, meaning we should use the level 2 data as the primary data for the stages from binning onwards; 2) level 1 data is the input for the IdePIX processor so, which provides additional quality flags to be added to the NASA level 2 flags for use at the binning stage.

The entire SeaWiFS GAC archive is available at PML. All SeaWiFS data are now public domain. The MLAC archive is also available at PML, though NASA OBPG have been collecting additional previously unavailable data donated from ground stations around the world, so these data may require an update at some point.

SeaWiFS level1 data can be found at:
oceandata.sci.gsfc.nasa.gov/directdataaccess/Level-1A/SeaWiFS (accessed October 2022)
SeaWiFS level 2 data can be found at:
oceandata.sci.gsfc.nasa.gov/directdataaccess/Level-2/SeaWiFS (accessed October 2022)

2.3 MERIS

For the purposes of the v6.0 ocean colour ECV dataset, the following MERIS data were used:

- Complete MERIS reduced resolution (reduced resolution; 1-km) level 1B global set (2002-2012) at the latest reprocessing level (4th reprocessing).

Access to MERIS data is available free of charge from ESA through the EO portal: earth.esa.int/eogateway/catalog/envisat-meris-reduced-resolution-geophysical-product-level-2-mer_rr__2p- (4th reprocessing as available at time of writing, accessed October 2022).

2.4 VIIRS

Data from two separate processing streams are freely available from NOAA and NASA OBPG, with the OBPG stream being preferable for C3S purposes. PML maintains an ongoing archive of level 1 data captured by the Dundee Satellite Receiving Station, covering most of Europe and some of the northern Atlantic. Sample data from the rest of the world are easily acquired from NASA OBPG's download site. Following the R2018.0 reprocessing (including conversion to netCDF), PML downloaded the complete level 2 archive. A full version of the level 1 archive also exists at PML and this was used to create L1C data for input to both POLYMER and IdePIX.

VIIRS level 1 data can be found at:
https://oceandata.sci.gsfc.nasa.gov/directdataaccess/Level-1A/SNPP-VIIRS (accessed October 2022)
VIIRS level 2 data can be found at:
https://oceandata.sci.gsfc.nasa.gov/directdataaccess/Level-2/SNPP-VIIRS (accessed October 2022)

2.5 OLCI

There has not been a single complete reprocessing of OLCI data, instead there are periodic reprocessing activities and ongoing updates to the 'baseline' processing. PML maintains a copy of the OLCI archive across the baselines as specified at https://www.eumetsat.int/ocean-colour-services (accessed October 2022). For this dataset the reduced resolution OLCI level 1 products were used.

The OCLI data used in this ECV processing were acquired using the API functionality at:
https://scihub.copernicus.eu (accessed October 2022).

2.6 Ancillary data — NCEP/ERA

The only other ancillary data required for the production of the ocean colour ECV are supporting data such as calibration tables and atmospheric measurements. Two primary data sources for atmospheric measurements are the National Centers for Environmental Prediction (NCEP)/National Center for Atmospheric research (NCAR) Reanalysis dataset (here after referred to as NCEP) and the ECMWF Reanalysis 5th Generation (ERA-5). NCEP is a continually updated (1948–present) globally gridded data set that represents the state of the Earth's atmosphere, incorporating observations and numerical weather prediction (NWP) model output from 1948 to present.

ERA-5 is the fifth generation of ECMWF atmospheric reanalyses of the global climate (climate.copernicus.eu/products/climate-reanalysis (accessed October 2022)). ERA5 Climate reanalysis gives a numerical description of the recent climate, produced by combining models with observations. It contains estimates of atmospheric parameters such as air temperature, pressure and wind at different altitudes, and surface parameters such as rainfall, soil moisture content, sea-surface temperature, and wave height.

Some of these are already held at PML (NCEP, attitude and ephemeris data for NASA sensors) and are automatically updated. Data from the ERA-Interim and ERA-5 reanalysis products have been downloaded up to the latest release date (at time of writing this is September 2022 for ERA-5).

2.7 In situ data

In situ data can be used for the vicarious calibration of sensors, development of product algorithms or algorithm assessment. The relevant in situ database used for algorithm assessment and intercomparison during the creation of this ocean colour CDR is the OC-CCI in situ database (see Figure 1). A full description of this dataset can be found in Valente et al (2022) and the DOI for the dataset is 10.5194/essd-2022-159. This dataset contains many in situ variables of use including chlorophyll-a and surface reflectance measurements. It is also of note that this is a compiled dataset that contains data from multiple other datasets.

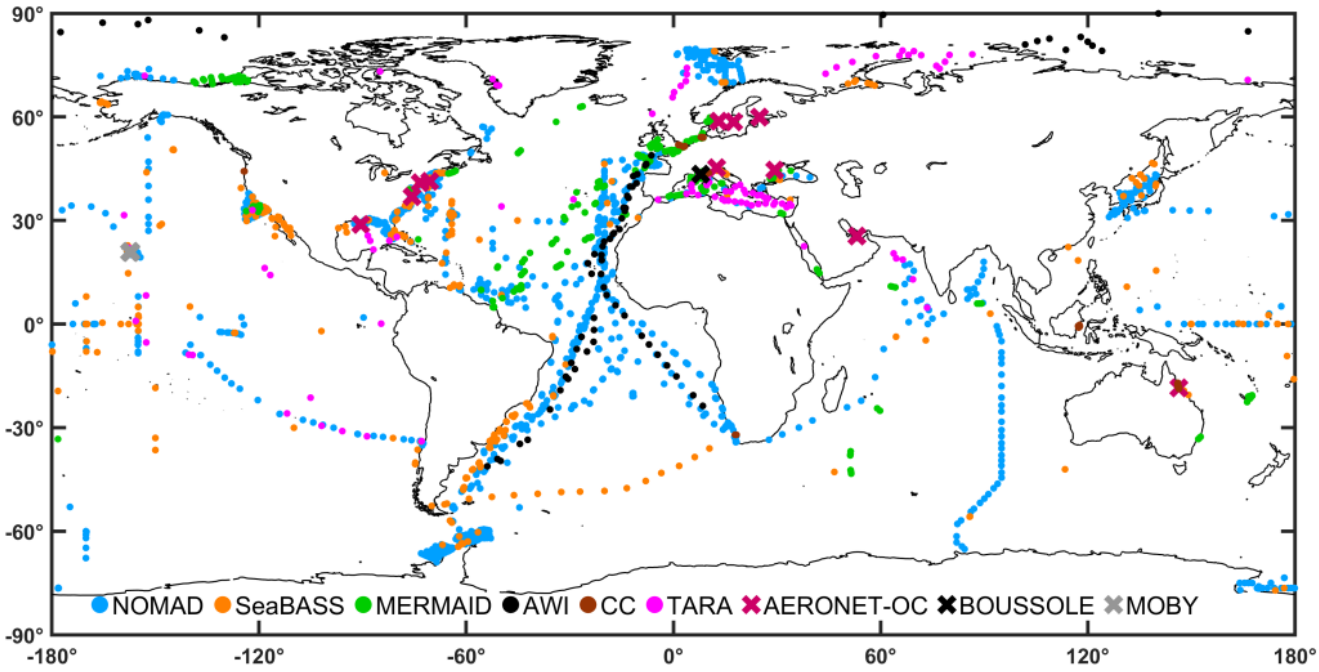

Figure 1: Global distribution of remote-sensing reflectance per input data set to Valente et al 2022. Crosses indicate time series and points are locations with at least one measurement. This is Figure 5 from Valente et al 2022.

3. Algorithms

3.1 Algorithm Fundamentals

3.1.1 Fundamental Concepts

Ocean colour remote sensing can be used for several applications and is an essential element to help understand and monitor the global marine ecosystem. Example applications of ocean colour data include:

- Mapping chlorophyll concentrations
- Estimation of inherent optical properties such as absorption and backscattering
- Estimation of phytoplankton physiology, phenology, and functional groups on large scales
- Monitoring of ecosystem changes resulting from climate change
- Detection of harmful algal blooms and pollution events
- Fisheries and recreational water management

Ocean color remote sensing from satellites began in 1978 with the Coastal Zone Color Scanner (CZCS). Following this “proof of concept” sensor, many other sensors have been developed and launched by organisations such as the National Aeronautics and Space Administration (NASA) and the European Space Agency (ESA). These sensors take measurements at multiple wavelengths, typically across the visible and near-infrared wavelengths (covering the 400 — 1000 nm range) with some wavelengths being primarily used for corrections or cloud detection rather than contributing directly to an output product.

Fundamentally, all passive ocean-color remote sensing follows the same principle. Sunlight enters a body of water and the spectral character of the sunlight is modified, depending on the absorption and scattering properties of the water. Some fraction of the modified sunlight makes its way out of the water and is detected by the remote sensing platform. The process of creating ocean colour products involves taking the radiance signal detected at the top of the atmosphere, retrieving just the signal from the water, and working backwards to deduce from the altered sunlight what substances (and at what concentrations) were present in the water.

This burying of information on the properties of the water within the radiance that returns from the water surface touches on the difference between Inherent Optical properties (IOPs) and Apparent Optical Properties (AOPs). IOPs are properties of a medium that are independent of the ambient light field in the medium. Put simply, IOPs are measures of the absorption and scattering properties of a water body. AOPs are optical properties that depend on the medium (the IOPs) and the geometric structure of the ambient light field. Common AOPs are reflectances, average cosines, and diffuse attenuation coefficients.

The International Ocean-Colour Coordinating Group (IOCCG) has published much helpful material on the fundamentals of ocean colour remote sensing, why it is important (see “Why Ocean Colour? The Societal Benefits of Ocean-Colour Radiometry” by Platt et al., 2008), and scientific working group reports on the evolving state of the art.

Though there are numerous variables that could fall under the remit of ocean colour, this dataset consists of just two, perhaps the most fundamental variables of ocean colour. The first variable available as part of this dataset is spectral Remote Sensing Reflectance. The second is Chlorophyll-a concentration.

Remote Sensing Reflectance, $R_{rs}(\lambda)$, has units of sr^{-1} (per steradian) and is reflectance of the surface waters at a number of visible wavelengths. More specifically it is the water-leaving radiance, corrected for bidirectional effects of the air-sea interface and sub-surface light field, divided by the downwelling solar irradiance, Ed(λ), just above the sea surface. R_{rs} is the primary variable of the Ocean Colour ECV and products such as chlorophyll-a are derived from the R_{rs} data.

Chlorophyll-a is a green pigment and the most prevalent photosynthetic pigment in both terrestrial and marine photosynthetic organisms. As an indicator of phytoplankton abundance, and therefore the base of the marine foodweb, chlorophyll-a concentration (chl-a) is recognised as an Essential Climate Variable. Oceanic chlorophyll-a is usually measured in units of mg m^{-3}, with concentrations ranging over multiple orders of magnitude.

It is worth noting that the process of retrieving high quality surface ocean information from the satellite signal can be a remarkably complex process. Just considering the number of factors effecting the radiance detected at the sensor highlights this. We need to consider Rayleigh scattering (air molecules), aerosols scattering, combined interactions of molecules and aerosols, ocean whitecaps, specular reflection of the sun (sun glitter), the actual water-leaving radiance we want to detect, the diffuse transmittances of the atmosphere, cloud effects, and contamination of the signal from nearby bright targets such as land or ice.

A further point of note is that there is often a distinction made in ocean optics between ‘Case-1’ and ‘Case-2’ waters. Case-1 waters are those where the optical properties are primarily correlated with chlorophyll-a, whereas in Case-2 waters the inherent optical properties can vary independently from chl-a due to high concentrations of other substances, such as sediment. Case-2 waters tend to be more coastal (or inland) and in these waters some of the assumptions used in a number of ocean colour algorithms do not hold true. There is no perfect line to draw between case-1 and case-2 waters however and within the production of this data record we have blended algorithms making use of knowledge of which waters they are most suitable for.

A useful and free resource for learning more about marine optics, ocean colour, and the complexities of remote sensing is the www.oceanopticsbook.info (accessed October 2022).

3.1.2 Overview of version development

This dataset is version 6.0 of the C3S Ocean Colour data. Recent improvements between the V5.0 and the V6.0 datasets include:

- Inclusion of the MERIS-4th reprocessing. V5.0 used the MERIS 3rd reprocessing.
- Addition of data from the Ocean and Land Colour Instrument (OLCI) aboard Sentinel 3B.
- We have upgraded the Quasi-Analytical algorithm (QAA) used in the band shifting to QAAv6 (the V5.0 data used the QAAv5).

- Minor update to the inter-sensor bias correction.
- MODIS and VIIRS data have been dropped from the record after 2019 due to concerns about the continued quality of data from the ageing sensors.
- Temporal extension of the record into 2022.

3.1.3 Algorithm Overview

The processing chain is founded on that of the Ocean Colour Climate Change Initiative (OC-CCI). Given that the processing chain uses a subset of available atmospheric correction schemes and in-water product algorithms (in order to maximise product quality) we undertake round-robin exercises to determine which algorithms to use at each of these stages. The round robin techniques are therefore also described here.

Input datasets

The input Earth Observation (EO) datasets were

- MERIS Reduced-Resolution (1km) L1b 4th reprocessing (including Offset Control Loop (OCL) fixes),
- MODIS level 1 data from NASA (R2018.0),
- R2018.0 level 1 VIIRS from NASA,
- SeaWiFS level 1 Local Area Coverage (LAC) (1km / Merged LAC: (MLAC), Global Area Coverage (GAC) (4km) R2018.0, and
- OLCI-3A and OLCI-3B L1b reduced-resolution data whose baseline number varies with date as covered at www.eumetsat.int/ocean-colour-services (accessed October 2022).

Atmospheric correction round robin

Multiple atmospheric correction schemes are compared in a round robin exercise (where the performance of each candidate algorithm is compared to that of all the other algorithms) for each of the sensors that is being used as input to the dataset. This round robin is updated when changes are made to either input level 1 datasets or atmospheric correction processor schemes. This round robin comparison is performed once to set the processor configuration and is not run within the processing chain shown in Figure 2.

Level 2 processing and binning

For all sensors except SeaWiFS, L1 data was processed with a POLYnomial based algorithm applied in the MERIS (POLYMER) algorithm (v4.14) to produce level 2 data. The principle of the POLYMER algorithm is a spectral matching method: it is based on (1) a polynomial used to model the spectral reflectance of the atmosphere and sun glint, (2) a water reflectance model and (3) the use of all available spectral bands in the visible. Further information is available in Steinmetz et al. (2011). SeaWiFS was processed to L2 using l2gen. The L1 data was also input to Identification of Pixels (IdePIX) (SNAP-6 version for all sensors except MERIS and OLCI which used SNAP-8 IdePIX) for the generation of pixel masks (such as cloud shadow and land) in addition to those provided through POLYMER processing.

All individual sensors were binned to level-3 4km (sinusoidal grid) with the SNAP binner. MERIS and OLCI were masked using IdePIX and POLYMER criteria. MODIS and VIIRS were masked using IdePIX,

POLYMER and NASA L2 flag criteria. SeaWiFS was masked using NASA L2 flag criteria and IdePIX. All available data were used, up to 31/12/2021.

Band shifting

Though the exact measurement wavelengths differ between ocean colour sensors, hence the need for band shifting, they are all chosen to align with significant absorption, scattering or fluorescence features of pigments or other optically active substances. More detail for MERIS is available at earth.esa.int/eogateway/instruments/meris/description (accessed October 2022). Within the band shifting module, SeaWiFS, MODIS, VIIRS and OLCI were band shifted to the six MERIS bands that are sufficiently close to band shift to (412, 443, 490, 510, 560, 665nm). This was performed by computing Quasi-Analytical Algorithm (QAA) estimates of Inherent Optical Properties (IOPs) and back computing the R_{rs} bands using a high-resolution spectral model. The output R_{rs} for 412-560nm were cleaned of any negative values, with the data items removed. Negative R_{rs} values in the 665nm band frequently occur due to low signal levels, and these were set to zero. As MERIS is the 'reference' sensor, no band shifting was required for MERIS data. MERIS was chosen as the reference sensor as 1) It is a historical and well characterized instrument, 2) it's wavebands align with the most recent sensors in the record (OLCI-A and OLCI-B), and 3) it directly overlaps with the other longer contributing sensors (SeaWiFS and MODIS).

Bias correction

Band shifted SeaWiFS and MODIS R_{rs} were corrected to remove gross differences (biases) against MERIS R_{rs}. The correction was done per-pixel using a temporally-weighted climatology windowed around the date being corrected, and using 7 day composites as input. This means that the bias correction factors vary per-day of the year and per-pixel, taking into account of seasonal and regional variations. These biases were computed over the 2003-2007 period with all sensors overlapping and functioning well. Bias adjustments were computed at locations where all sensors had valid data, with a temporal window of ± 45 days (weighted by time difference from the center point) and spatially-limited interpolation (11 pixels) to fill smaller gaps. VIIRS and OLCI 3A are then also corrected to MERIS levels by a similar process but comparing against MODIS-corrected-to-MERIS-levels rather than directly to MERIS. This indirect comparison is unavoidable due to the lack of temporal overlap. Finally, OLCI 3B is corrected to the MERIS-like OLCI 3A record.

Merging

Following de-biasing, the individual sensor data were merged with a simple average.

Water class membership

Water class memberships are measures of how closely, in a spectral reflectance sense, the waters in a given pixel resemble each member of a set of pre-defined optical water types. Here, water classes were computed following Moore et al (2009), with (14) specific water classes derived from the v6.0 R_{rs} values (Jackson et al. in prep) using a methodology developed from that of Jackson et al. 2017. The set of classes was derived by a process that iteratively adds new classes. Each iteration identifies poorly classified pixels from a training dataset, and then creates candidate classes for those spectral sets.

In-water algorithm round robin

Given the range of available algorithms for deriving in-water products such as chlorophyll-a, it is necessary to perform an inter-comparison assessment to see which algorithms are best suited for use with the band-shifted, bias corrected and merged R_{rs} products. This is performed such that algorithms are assessed using matchups against in situ measurement and per optical water type. This means that the performance of each algorithm is assessed for each of the optical water types that are defined for the water class membership calculations. This allows multiple algorithms to be used within the processing chain, but blended so that they only contribute to the final in-water products when they are known to perform well. As with the atmospheric round robin, this is performed once to set the processor configuration and is not run within the processing chain shown in Figure 2.

Product generation

A range of products were computed from the merged R_{rs}, directly using the validated algorithms in the SeaWiFS Data Analysis System (SeaDAS(v7.5)). Algorithms were selected from the best performers in the round-robin evaluation:

- Chlorophyll: blended merge of OCI, OCI2, OC2, OC3, Ocx and OC5, weighted by the relative levels of membership in specific water classes.

Re-projection

All data are re-projected onto a geographic grid in addition to the basic sinusoidal grid (this has less bins per horizontal strip of latitude due to the fact the earth is a sphere, it does not distort the spatial representation of the poles like geographic projection does). The re-projection engine is that from the Sentinel Applications Platform (SNAP) software. Both projections have Ocean Colour Climate Change Initiative (OC-CCI) style metadata added which follows Climate and Forecast (CF) Metadata Conventions.

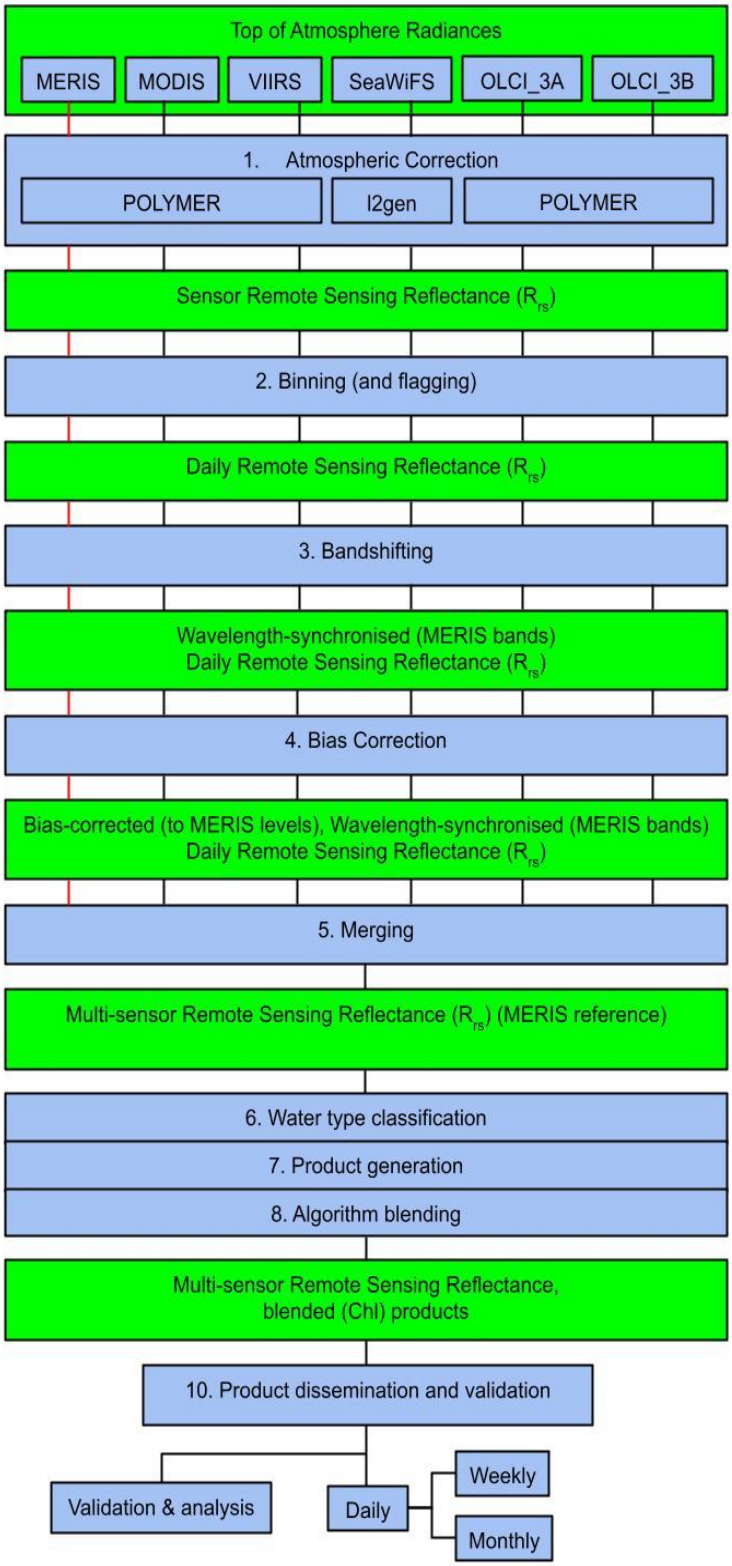

Figure 2: Data flow in the Ocean Colour ECV production process. Note that the atmospheric round robin is not part of the processing chain. It is performed once prior to the main data processing and the results are used to build the final processor configuration. As such it is not shown here as part of this process.

As shown in Figure 2, there are multiple stages in the ocean colour processing chain. Below we cover each stage in turn, describing its function and implementation. As described in the Algorithm fundamentals section, the data are put onto a common grid for merging in the 'binning' stage. All processing prior to this is performed at the native resolution of the input Level 1 or level 2 data.

3.2 Atmospheric correction

3.2.1 Atmospheric correction round robin

A round robin comparison is one in which each candidate is compared against all other candidates. In the context of the atmospheric correction for ocean colour this assessment was performed individually for each sensor. The round robin assessment is performed using match-ups against in situ data and a multi-metric scoring approach, which is described below.

3.2.1.1 In situ data

The round robin makes use of match-ups of remote sensing and in situ datasets. These in situ match-ups are normalised, band-shifted (if required), and quality checked in order to remain equivalent to the remote sensing data. All case-1 like spectra (based on the Lee case 1 definition - see OC-CCI PVASR-v3.0, section 2.2, and Lee and Hu, 2006) are normalised using the fQMorel method and for others (i.e. case-2) the methodology of Park and Ruddick (2005).

The process of correcting for the bi-directional variation in reflectance is a complex matter. However, in brief, the Morel and Gentilli approach is based on the use of lookup tables to provide values of the f/Q ratio in all the necessary conditions, where f relates $R(\lambda)$ to backscattering and absorption coefficients, and Q is the ratio of upwelling irradiance to any upwelling radiance. The f/Q ratio is dependent on the geometric configuration (solar zenith, sensor zenith, and relative azimuth), λ, and the bio-optical state, depicted by Chl. The Park and Ruddick approach also uses a remote-sensing reflectance model based on a lookup table. Model coefficients depend on three angles—solar zenith, sensor zenith, and relative azimuth—to take account of directional variation, but then a phase function parameter is used to define the contribution of suspended particles to the backscattering coefficient.

Matchups for case-1 and case-2 are analysed separately and as combined datasets.
The band shifting approach is described later in this document but in summary:

- The band shift uses all bands in the input spectrum.
- The models for the estimation of chlorophyll concentration and IOPs follow the parameterisation by Zibordi et al (2009), but representative coefficients are derived directly from the OC-CCI in situ data. Mainly the NASA bio-Optical Marine Algorithm Dataset (NOMAD) provides simultaneously IOP and R_{rs} measurements (normalised with fQMorel).
- During band-shifting, the models are selected based on radiometric properties (reflectances) alone which allows for variability of water classes at single sites.

3.2.1.2 Candidate Atmospheric correction algorithms

Atmospheric correction processors considered are:

- MEGS v8.1
- l2gen v7.3.2
- C2Rcc v0.15

- POLYMER v4.0

All four algorithms could be applied for the MERIS sensor only as there is no version of MEGS for the other sensors. For SeaWiFS, MODIS, and VIIRS three processors could be tested. MODIS, SeaWiFS and VIIRS are processed to L1c for all processors so that radiometric corrections are applied correctly to the data. For the final processor configuration (following the round robin results) see section 1.2.

3.2.1.3 Matchup-QC

Matchup extraction returns a macro pixel (three by three pixels) centered on the in situ data. The satellite overpass and the in situ measurement have to occur within a ± 3 hours time difference. If more than one in situ measurement at the same location are available only the one closest in time is considered.

A match-up, after atmospheric correction (AC) and IdePIX flagging (available as a SNAP software plug-in), must also pass the following checks (performed for each wavelength independently):

- An outlier filter in form of a standard deviation (σ) from mean (μ) filter is applied to the remaining pixels per wavelength in the macro-pixel. Valid pixels must fulfil the following criteria for all wavelengths (independently) with f =1.5 :

$$\mu\lambda - f \cdot \sigma\lambda \leq \mathrm{R}rs_{\mathrm{n}}(\lambda) \leq \mu\lambda + \mathrm{f} \cdot \sigma\lambda \qquad (1)$$

- The number of valid pixels must be greater than half of the size of the macro pixel.
- The macro pixel must be relatively homogeneous ($\sigma\lambda / \mu\lambda < 0.15$).

3.2.1.4 IBQ and CBQ

For algorithm inter-comparison, it is common practice to restrict analysis to a common data pool (matchups available for all processors in this case). However, this approach achieves an incomplete picture. Therefore, tests are performed for a set of common best quality (CBQ, pixel flags are merged across processors so only pixels valid for all processors are considered) pixels and for sets of the individual best quality (IBQ, all valid pixels for a given processor). CBQ might be considered a fairer assessment of algorithms as it considers only points valid for all. In contrast, IBQ is an assessment of the products as they would be after processing (not filtered by other algorithms flagging). As such, the first approach gives a comparison of potential qualities, while the latter is much closer to practical applications of this processor. Note that the homogeneity criterion can still lead to a different amount of available good match-up points in the CBQ case as it is dependent on the noise rather than processor pixel flags.

3.2.1.5 Statistics and Scoring

The Round robin exercise is a multi-metric assessment, making use of:

- Root Mean Square Error
- Bias (absolute)
- residual error (absolute)
- $\chi 2$

The statistics are assessed per wavelength, except for the χ2 value, which is based on five wavelengths as it is a spectral property. In all cases the lower the metric the better the algorithm is performing. The algorithms are scored for each metric as follows:

- The best algorithm receives 2 points.
- Algorithms where metrics fall within the confidence interval of the best receives 2 points.
- Algorithms with overlapping confidence intervals with the best (but not having the mean statistic falling with the interval of best) receive 1 point.
- If the confidence interval of an algorithm does not overlap with the best algorithm, this algorithm receives 0 points.

The scores are then normalised so that the sum of all points per wavelength and property over all algorithms equals 1.

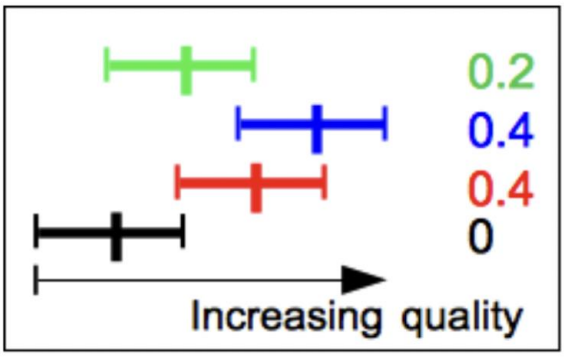

Figure 3: Example of the scoring scheme after normalisation to 1. The highest quality (blue) is followed by a not significantly lower (red), and significantly lower but with overlapping (green) and not overlapping error bars(black).

All scores (S) are then summed up per wavelength (*i*) and statistical property which gives each of them equal weight. The measure of spectral shape, i.e. the mean χ^2 value, receives the same weight as a single waveband. The score for spectral shape is therefore multiplied by three when added up to a total score because there are three statistical parameters considered per wavelength.

$$S_{total}(processor) = \sum^{7i} S_{RMSE.abs}(\lambda_i) + S_{res.error}(\lambda_i) + S_{bias}(\lambda_i) + 3\,S\chi^2 \qquad (2)$$

where each subscript on *S* refers to a different metric.

In order to give a robust conclusion from the inter-comparison and scoring, the assessment is also performed using a bootstrapping (Efron, 1979) approach. This produces a distribution of scores for each of the processors which is assessed in the final determination of the optimal algorithm.

3.2.2 Current Atmospheric correction configuration

The atmospheric correction stage is intended to produce values for the remote sensing reflectance (R_{rs}) at the ocean surface. In the v6.0 chain POLYMER (Steinmetz et al 2011) was used to perform atmospheric correction for all sensors apart from SeaWiFS. For a detailed description of the algorithms used in these processors, see the specific POLYMER ATBD[1]. POLYMER Source code is currently available within the C3S consortium and to ESA (presumably also to suitably contractually bound organisations nominated by ESA) but has licensing conditions attached that prevent further distribution. POLYMER accepts a configuration file that specifies many parameters used within the algorithm. This configuration file also specifies the input and output filenames. In the POLYMER version (4.14) used here, masking (pixel identification) is included, in particular masking of cloud, snow and ice, long atmospheric pathlengths and algorithm failures. The masking is applied at the binning stage.

L1A data as used for, for example, MODIS and VIIRS first runs through a sensor calibration step. Since L1A data comprises the original charged-couple device (CCD, this the type of sensor using in most digital imaging) counts, sensor and vicarious calibrations involve adjusting the coefficients used to transform the counts for each channel into physical top-of-atmosphere radiances, referred to as L1B data. Data for MERIS, and also for OLCI, are supplied pre-processed to L1B. This saves some processing effort and spares the user from having to deal with calibration-specific characteristics, but also prevents the user from adjusting the calibration to deal with any L1A processor errors. L1B data are then input first to sensor-specific radiometric correction (e.g. correction for MERIS Smile-effect) followed by (i) a classification of each pixel as land, water, cloud and (ii) the atmospheric correction (AC). For water pixels, the application of an AC results in water-leaving reflectances from top-of-atmosphere L1B radiances.

In addition to the flags generated within the POLYMER and L2gen processors, additional flags are required to ensure that final data quality remains of sufficient quality for climate studies. IdePIX[2] is a pixel classification tool which takes L1B/C data as input. IdePIX was applied alongside POLYMER/L2gen flags to generate a complimentary set of pixel flag products for all sensors. For all NASA sensors (MODIS, SeaWiFS and VIIRS) flags were also pulled from the L2 (SeaDAS[3] generated) products even if POLYMER was the primary processor. One additional point of note is that it was noticed during the quality control exercises that the MLAC (1km resolution) SeaWiFS data was noisy in close proximity to cloud masked pixels in some regions (due to unmasked straylight and cloud shadows). In order to maintain final product quality we expanded the MLAC STRAYLIGHT and LOWLW flag using a binary dilation[4]. The applied flag set is summarised in Table 2.

[1] https://docs.pml.space/share/s/M05k8Lw3QLeXSIiA3X87UQ (accessed October 2022)
[2] https://www.brockmann-consult.de/portfolio/idepix/ (accessed October 2022)
[3] https://seadas.gsfc.nasa.gov (accessed October 2022)
[4] https://docs.scipy.org/doc/scipy-0.16.0/reference/generated/scipy.ndimage.morphology.binary_dilation.html (accessed October 2022)

Table 2: Flags applied during the binning of level 2 processed data.

Sensor	POLYMER FLAGS	IDEPIX FLAGS	L2GEN FLAGS
SeaWiFS	N/A	INVALID, CLOUD, LAND, SNOW_ICE, CLOUD_BUFFER, CLOUD_SHADOW	CLDICE COCCOLITH, CHLFAIL, NAVWARN, FILTER, HIGLINT, LOWLW, HILT, MAXAERITER, HISOLZEN, HISATZEN, NAVFAIL, ATMFAIL, STRAYLIGHT, LAND
MERIS	(bitmask & 1023) ==0, (Rnir - Rgli) $\leq$ 0.027	INVALID, CLOUD, LAND, SNOW_ICE, CLOUD_BUFFER, CLOUD_SHADOW	
MODIS	(bitmask & 1023) ==0, (Rnir - Rgli) $\leq$ 0.027		LAND, CLDICE
VIIRS	(bitmask & 1023) ==0, (Rnir - Rgli) $\leq$ 0.027	INVALID, CLOUD, LAND, SNOW_ICE, CLOUD_BUFFER, CLOUD_SHADOW	STRAYLIGHT, ATMWARN, CLDICE
OLCI-A	(bitmask & 1023+2048+4096+8192) ==0, Rnir $\leq$ 0.1, Rgli $\leq$ 0.1	INVALID, CLOUD, LAND, SNOW_ICE, CLOUD_BUFFER, CLOUD_SHADOW	
OLCI-B	(bitmask & 1023+2048+4096+8192) ==0, Rnir $\leq$ 0.1, Rgli $\leq$ 0.1	INVALID, CLOUD, LAND, SNOW_ICE, CLOUD_BUFFER, CLOUD_SHADOW	

SeaDAS is the processing software made available by NASA's OBPG (as NASA L2 data were used the relevant SeaDAS version should be SeaDAS v7.5). As an externally maintained (and extremely complex) component, SeaDAS is not described in this document. The source code for SeaDAS is freely available. As a work of the US government, there is no copyright and thus no restrictions on any use. There is some documentation online at OBPG's website[5].

The intermediate L2 product therefore comprises the outputs of the pixel classification (surface type flags) and the output of the atmospheric correction (water-leaving reflectances and flags). Following the acquisition or generation (depending on the sensor) of level-2 atmospherically-corrected radiances, the data are binned onto a common grid for further processing. Note that as the final output of the ECV processing chain is a multi-sensor merged product, we must interrupt the 'standard' full level-1 to level-3 processing chain, to include steps for harmonising wavelengths (bandshifting) and bias correcting between sensors, before merging multiple sensor data into a single product. In-water products (Chlorophyll-a) are then generated from merged reflectances. The C3S processing also deviates from that of a single sensor by converting to a binned product

[5] http://seadas.gsfc.nasa.gov/ (accessed October 2022)

(effectively an L3 product) after atmospheric correction and prior to merging. This approach was chosen partly to simplify the merging algorithm and its input data requirements and partly to control data volumes.

3.3 Binning

The merging processor requires its input data to be in the form of an integerised sinusoidal grid, as shown in Figure 4. This is a psuedocylindrical equal-area projection (sometimes referred to as the Mercator equal-area projection). The grid used for binning the level2 data has an approximate grid dimension of 4.64km (referred to as a 4km product), contains 4320 latitudinal rows and a total of 23,761,676 bins across the globe. This grid projection is chosen as it more accurately represents the physical area occupied at different latitudes, whereas the more common/simpler geographic projection leads to a statistical misrepresentation of the importance of the areas north/south of the equator, especially at the poles. The grid is actually stored as a 1D array of bins, with coordinates of each bin stored alongside the bin. This data format is sparse – i.e. bins containing no data are simply omitted from the output. It is well described in the Product User Guide (PUG) document (C3S2_PUGS). This is also the same gridding style used by NASA for their level-3 binned data.

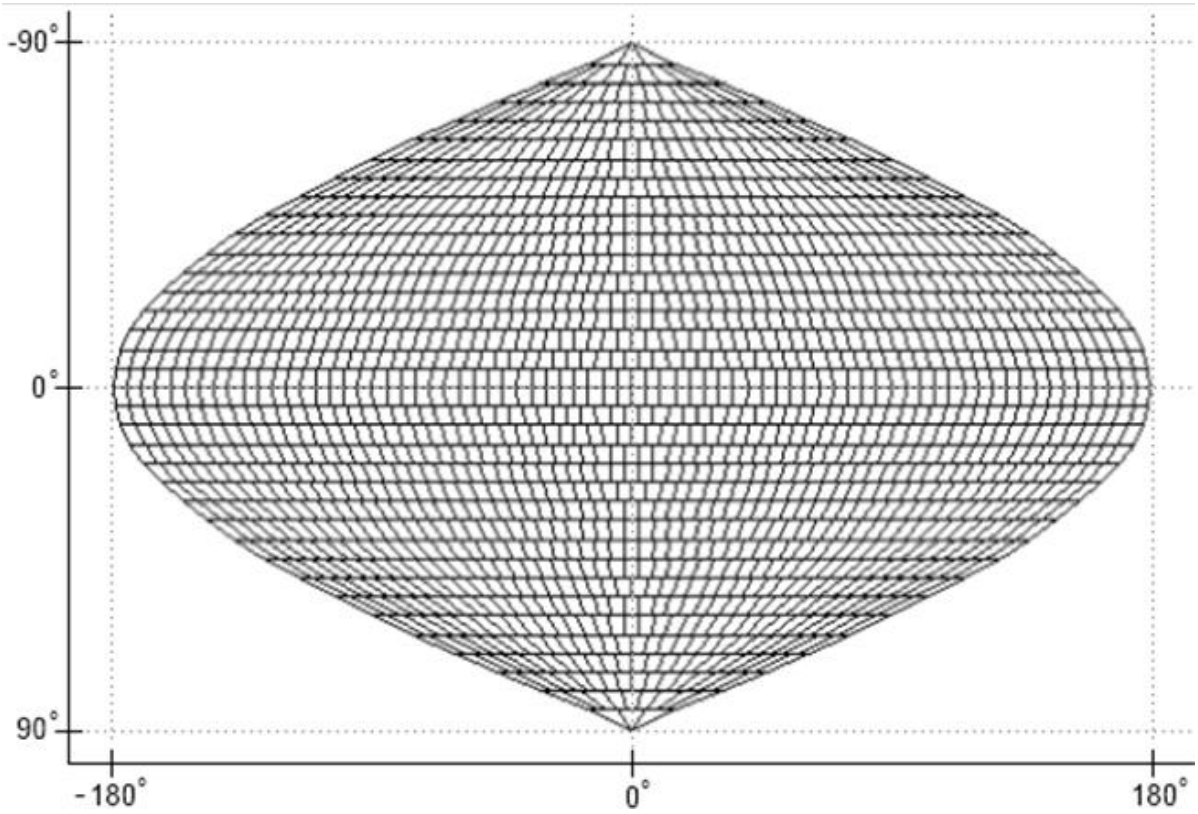

Figure 4: An example of a sinusoidal, equal area grid. This maintains a consistent area per pixel without significant distortion towards the poles as is seen in geographic projections.

In v6.0, all of the input datasets (POLYMER processed MERIS, VIIRS, MODIS and OLCI and the L2gen processed SeaWiFS) must be binned from level 2 (satellite projection, with 2D arrays of data with matching latitude and longitude for every cell) to this NASA-style L3bin format[6]. The binner samples

[6] https://oceancolor.gsfc.nasa.gov/docs/format/l3bins/ (accessed October 2022)

at a higher resolution than the output to reduce the incidence of edge-of-swath pixels being spread out with gaps in between (the "speckle" effect noted in some areas) for all sensors. This is particularly important for sensors with wider swaths (e.g. VIIRS), and there was some additional tuning required to optimise interpolation distance.
An important point for SeaWiFS is that GAC is a 1/16 subset of LAC but is globally available (GAC was small enough to be recorded on the satellite and downlinked, while LAC was only available when the satellite was in range of a ground station). This means that any LAC data necessarily includes pixels that are present in GAC. Double-counting is avoided by blanking out GAC data when LAC are present and is done on a line-by-line basis. Identical lines are recognised by the per-line timestamp in the input files.
Rather than re-implement another binner, the SNAP v6.0 binner developed by Brockmann Consult[7] was used to produce these data. As the merging processor needs R_{rs}, but POLYMER outputs Rw, the SNAP band math facility is used to divide Rw by π in the same process as binning. The algorithms used in the binner are standard and are described in the BEAM online documentation[8] where access to the source code is also available.

While it would be expected that filtering due to features such as clouds or sunglint, would happen at level 2, it actually occurs during the binning stage as a pre-filtering step (still at level 2 but integrated into the binning process). The processing engine used is the SNAP[9] binner. In addition to the band math, an extra step aggregates the masks from IdePIX (where available), NASA L2 flags (if required) and the level 2 POLYMER processed product, then uses all the aggregated masks in the binning step.

3.4 Band shifting

Full details and assessment of this approach are given in the OC_CCI-ATBD on Data Bias Correction and Merging[10] document but we have given the main details of the approach below.
The band shift correction aims at expressing R_{rs} at a target wavelength λ_t from its values at a set of input wavelengths λ:

$$R_{RS}(\lambda_t) = BS[(R_{RS}(\lambda), p], \qquad (3)$$

BS being the band-shift correction function and *p* a set of parameters.

Besides purely statistical or empirical approaches, a way to express R_{RS} at one wavelength from a set of wavelengths relies on the relationship between R_{RS} (apparent optical property, AOP) and its inherent optical properties (IOPs). This is supported by the fact that IOPs have spectral shapes that are fairly well known, at least within certain bounds of natural variability. They can thus be used as predictors of the R_{RS} spectral shape. Assuming that the total absorption *a* and back-scattering b_b coefficients are known at 2 different wavelengths λ and λ_t, the corresponding R_{RS} values can be linked by an expression of the type:

[7] https://www.brockmann-consult.de (accessed October 2022)
[8] http://www.brockmann-consult.de/beam/doc/help/index.html (accessed October 2022)
[9] https://step.esa.int/main/download/snap-download/ (accessed October 2022)
[10] https://docs.pml.space/share/s/2RVhiuK2SWyhbSthqDDoxg (accessed October 2022)

$$R_{RS}(\lambda_t) = R_{RS}(\lambda)\frac{f(\lambda_t)}{Q(\lambda_t)}\frac{Q(\lambda)}{f(\lambda)}\frac{b_b(\lambda_t)}{a(\lambda_t)}\frac{a(\lambda)}{b_b(\lambda)} \quad (4)$$

or alternatively:

$$R_{RS}(\lambda_t) = R_{RS}(\lambda)\frac{f'(\lambda_t)}{Q(\lambda_t)}\frac{Q(\lambda)}{f'(\lambda)}\frac{b_b(\lambda_t)}{a(\lambda_t)+b_b(\lambda_t)}\frac{a(\lambda)+b_b(\lambda)}{b_b(\lambda)} \quad (5)$$

where *f* and *f'* relates apparent optical properties (irradiance reflectance) to IOPs, and Q is the ratio of irradiance and radiance just below the surface (Morel and Gentili, 1991, 1996).
Only the dependence on wavelength is made explicit in Eqs. (4-5). Particularly the dependence on geometry is not written. For operational products, it can actually be assumed that R_{rs} is "fully normalised", and that bi-directional effects have already been dealt with. The effect of the passage through the air-sea interface is assumed to be spectrally invariant with a good accuracy. The ratios f/Q and f'/Q are weakly variable with wavelength at least over short spectral intervals. For validation or inter-comparison exercises, they have been assumed to be spectrally invariant (for λ close to λt), or parameterised as a function of Chl-a within a Case-1 water hypothesis (Morel et al., 2002), which might result in varying levels of uncertainty across different optical water types. Specifically, a parameterisation of f/Q (or f'/Q) that would be applicable to optically complex waters is still lacking (even though some progress is being made, e.g., Park & Ruddick, 2005).

In any case viable estimates of *a* and b_b are required, which means that an algorithm is needed to calculate these coefficients from the input R_{rs}. The latest OC-CCI IOP round-robin comparison identified the Quasi-Analytical Algorithm (QAA, Lee et al., 2002, updated to the QAA_v6) as the optimal IOP algorithm to be used for the band shifting. This utilises the v6.0 (2015) configuration of the QAA algorithm[11], with corrections for raman scattering (IOCCG,2017). Therefore, Eqs 4-5 are substituted by the QAA relationship between R_{Rs} and IOPs. It is worth noting here that this relationship is also based on assumptions about the spectral shape of some absorption and scattering properties and the transmission across the sea surface (even though not specifically associated with a Case-1 water type).

The strategy is then to derive a set of IOPs using the QAA (inversion mode), convert these IOPs at the desired wavelength λ_t using spectral shapes assumed in the QAA, and expressing R_{rs} at λ_t using the QAA in forward mode. It is worth emphasising that the spectral shapes of *a* and b_b are more important than their actual amplitudes since the method works essentially through ratios.

3.5 Bias Correction

Various studies have shown that the bias between missions can be significant and may vary in space and time (e.g., Djavidnia et al., 2010, Mélin 2011, Zibordi et al., 2012a,b). It has also been shown that, if not corrected, inter-mission biases can significantly alter trend analyses performed on multi-mission combined products (Mélin, 2016). C3S2 follows the OC-CCI project approach to reduce the bias between sensor-specific products as much as possible; while acknowledging that a residual bias is unavoidable.

[11] http://www.ioccg.org/groups/Software_OCA/QAA_v6_2014209.pdf (accessed October 2022)

As mentioned above, there are significant differences between sensor-specific R_{rs} products. Even after using the same atmospheric correction processor and long-term averaging, some differences are still visible. For instance, MERIS R_{rs} appears lower than R_{rs} associated with SeaWiFS or MODIS in the south subtropics and higher in the subarctic regions. The spatial global average of R_{rs} also shows some perceptible differences even though there is an overall consistency.

The principle of the bias correction scheme results from the requirements of operating the bias correction every day and referring to bias maps that vary along the annual cycle. The selected approach is to pre-compute daily bias maps that are easily applied for each day being processed. The approach used is to construct the bias correction maps including only matching pairs of R_{rs} values (i.e., from 2 missions). The merit of this selection is to build the bias correction only on coincident data from two missions, which should lead to more accurate bias estimates. However, it must be noted the drawback is a large reduction of the number of available samples to construct the bias correction.

The approach implemented in v6.0 begins with a rolling temporal averaging of daily products as a pre-processing stage, before computing daily ratios of comparative and reference sensor data. The purpose of the pre-processing step is to improve “density” and smoothness of bias maps. As there is no direct temporal overlap between some sensor pairs (i.e. MERIS and OLCI) there is a second cycle of the bias map creation. Thus, the first part of the bias correction routine now refers to three sensors: SeaWiFS, MERIS and MODIS, and the second part described afterwards targets MODIS, VIIRS and OLCI.

Considering two missions, one being the mission selected as reference, the bias map creation steps are as follows:

1. For each daily product over the reference periods 2003-2007 (sensor pairs in part 1) or 2012-2019 (sensor pairs in part 2), for each sensor, a rolling temporal average (mean value) map of R_{rs} is calculated over the period of 7 days: the data day itself plus 3 days before and 3 days after.
2. For each day, all matching pairs of R_{rs} are identified, and their ratio (δ) is calculated (Eqn 6): where again *ref* and *i* designate the reference mission (taken as MERIS) and the mission to be corrected, respectively, the ratio being expressed at wavelength λ, for the bin location *b* and the day *d*. Note that “each day” now implies that the product includes averaged data from the surrounding 7 days.

$$\delta_i^{ref}(\lambda, b, d) = \frac{R_{rs}^{i}(\lambda, b, d)}{R_{rs}^{ref}(\lambda, b, d)} \quad (6)$$

3. A daily climatology of the ratios δ (i.e., 365 files) is produced for each pair of missions over the period of reference 2003-2007 or 2012-2019. At this stage, the daily climatological values (based on X years of available overlap data) result from the averaging of X daily maps (i.e., up to 5 values of R_{rs} ratios for each grid point in the 2003-2007 overlap period). These ratio climatology maps have a variable spatial coverage, or conversely a limited temporal sampling at each grid point (not every pixel will have a value in the climatology map for every day of the year), which does not appear suitable for a bias correction to be applied to any data day.

4. The next step creates a smoothed series of daily values by operating a weighted average over a temporal window of 2N+1 days (±N days before and after the considered day): Smoothing of the daily climatology over a temporal window of 2N+1 days with the smoothed value <δ(d)> at day d being (dependencies other than the day number are dropped):
5.

$$< \delta(d) > = \frac{\sum_{i=-N}^{N} w_i(\delta)(d+i)\theta_i}{\sum_{i=-N}^{N} w_i \theta_i} \quad (7)$$

with

$$w_i = \frac{N+1-|i|}{N+1} \quad (8)$$

and θ_i=1 if δ(i) is associated with a valid value, 0 otherwise. The weights are thus 1 for the same day of the climatology, N/(N+1) for the days before and after, and 1/(N+1) for the first and last days of the ±N-day window. In the creation of the v6.0 dataset N is set to 45 days, a number derived through testing of coverage gain with temporal window length where a desire for a shorter time window is balanced against the need for coverage.

6. Spatial interpolation is used to fill in empty grid points in daily bias maps. It was decided that a pixel should be interpolated using data from at least 5 local pixels. Initially a 3x3 grid around the missing pixel is interrogated and if sufficient valid pixels are found then the missing pixel is filled with the weighted mean of the 3x3 grid. Pixels are deemed invalid if they contain no data or fall within a predefined landmask. If sufficient valid pixels are not found, the grid is expanded to 5x5 and so on until 5 pixels are found. To ensure that only local data were used, an upper limit was set for the grid size at 11x11. Averaging gives more weight to pixels closer to the central point with the following formula:

$$< x > \frac{\sum_{d=1}^{5} \sum_{i=1}^{8d} \frac{1}{d} \theta_{d,i}\, x_{d,i}}{\sum_{d=1}^{5} \sum_{i=1}^{8d} \frac{1}{d} \theta_{d,i}} \quad (9)$$

where *d* is the distance from the central point (e.g., *d*=1 for the ring of side 3 surrounding the center), $\theta_{d,i}$ is equal to 1 if there is a valid value, 0 otherwise, and $x_{d,i}$ is the associated value. This can be envisioned as sequentially searching larger rings of pixels around the empty pixels. A ring being at a distance d from the central point has a side length of 2d+1, and contributes a number of points of 4 times 2d, hence the 2nd summation in Equation (9). The summation on d can be stopped before d=5 (i.e., a ring of side 11) if at least 5 valid values have been detected. A diagram showing this for the first 2 rings is shown in Figure 5.

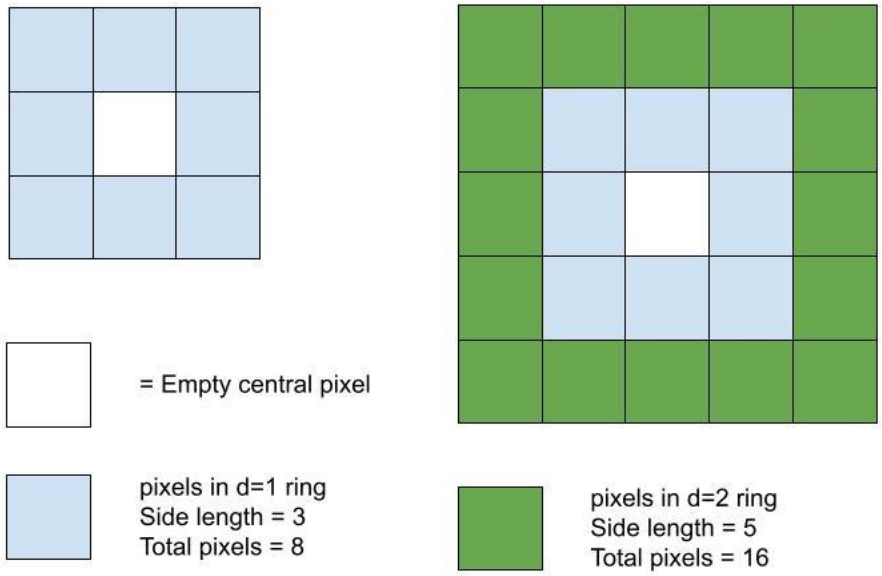

Figure 5: diagram showing the increase in pixels searched for data in stage 5 of bias map creation.

Once the bias maps are created, the bias correction of sensor data for a given pixel is then the reverse operation applied on any daily R_{rs} record at bin location *b* and day *d* to produce a bias-corrected R_{rs}:

$$R_{rs}^{i,corr}(\lambda, b, d) = \frac{R_{rs}^{i}(\lambda, b, d)}{< \delta_i^{ref}(\lambda, b, d) >} \quad (10)$$

Equation (10) is applied only if there is a valid value for $<\delta_i^{ref}(\lambda,b,d)>$ (described in equation 6 above); otherwise, the reflectance value is set to missing. This results in a minor loss of data but is preferred with respect to including uncorrected values in the data record.

From this point, a second stage is performed to correct the VIIRS and OLCI data to MERIS-equivalent levels by aligning it with the already-corrected MODIS data. Therefore, the routine described above is reproduced using MODIS R_{rs} corrected as the reference. The reference period is potentially from 2012 onwards, but the length of overlap with VIIRS and OLCI differs greatly. As the most recent data may be of lower quality than consistently reprocessed data, the total overlap period was not used. Instead for MODIS and VIIRS the years 2012-2014 were used and for OLCI 3A July 2016 - July 2019 were used. The bias correction of OLCI 3B is performed against the corrected OLCI 3A. This is due to degradation of the MODIS sensor in recent years, meaning that the limited flight time of OLCI 3B would make comparison to MODIS overlap potentially risky. Instead the overlap period between OLCI 3A and 3B (July 2018-July 2021) is used to bring 3B in line with the MERIS-reference record. Note there is a quality control check performed on the value of the bias. It appeared that in a very few cases, δ_i^{ref} could be very low, resulting in very (even unrealistically) high corrected reflectance.

To reduce the possibility of such occurrences, thresholds are enforced so that $\delta_{min} < \delta_i^{ref} < \delta_{max}$ where δ_{min} and that δ_{max} are set using 1st and 99th percentiles of bias ratios across the time series. Still, these restrictions on the δ values might not suffice to prevent unrealistically high R_{rs} values after application of Equation (10). Therefore, as a final step, spectra are excluded if the resulting (bias-corrected) R_{rs} value appears greater than $1/\pi$ (sr^{-1}) as ocean reflectance this bright (>30%) is extremely unlikely.

The scheme outlined above relies on 366 bias maps for each band and each sensor pair. For the date of 29th February during leap years, the average daily maps of δ are computed taking the mean of the maps associated with 28th February and 1st March.

3.6 Merging

One of the primary requirements in creating a CDR is that we must merge data from multiple sensors in order to have a record that has a sufficiently long temporal extent to detect climate signals. Assuming that the inputs to the merger are now band-shifted and bias-corrected reflectances, the merging can proceed with a weighted averaging. This approach has advantages (see related [OC-CCI-ATBD-DBCM] document on merging techniques) which include speed of calculation, robustness, and a clear statistical interpretation. The final expression for the merged product is:

$$x = \frac{\sum_{i=1}^{m} \theta_i w_i x_i}{\sum_{i=1}^{m} \theta_i w_i} \qquad (11)$$

where the sum is made over the *m* sensors, x_i is the input for each sensor, θ_i is a presence function for sensor *i* (equal to 1 if there is a value associated with sensor *i*, 0 otherwise), and w_i is the weight for sensor *i* at the considered bin. Currently, for the production of Version 6.0 data, the weights have been defined as 1. However this could be changed in the production of future versions if needed, to reflect information on the number of pixels associated with the considered bin for each sensor, and/or the uncertainty associated with the datum from each sensor, or in general an index of quality. Note that large negative values are filtered out for most bands (665nm is a notable exception due to its low signal levels). The averaging is accompanied by a compilation of each sensor's presence as a dedicated variable (called 'index'). This information can then be propagated through time compositing.

3.7 In-water algorithms (Derived Products) and Algorithm Blending

The previous section has described the production of Rrs values. These are available at a spatial resolution of 4km, a temporal resolution of daily, and geolocated on the sinusoidal equal area projected grid. Here, we describe the calculation of Chl-a estimates from the Rrs values.

3.7.1 In-water algorithm round robin

3.7.1.1 In situ Dataset

As with the atmospheric correction inter-comparison described above, the in-water round robin inter-comparison makes use of a pre-existing, curated database on biological oceanographic data collated through the OC-CCI project (Valente et al 2022). This database contains hundreds of variables (such as spectral absorption, spectral reflectance and chlorophyll-a concentration). For

this work the variables used were the High Performance Liquid Chromatography (HPLC) and turner fluorometry (extracted chlorophyll-a) based chlorophyll-a measurements. If both fluorometric and HPLC data were available for the same location and time (synchronous measurements taken) then the HPLC was used as the preferred measurement method.

3.7.1.2 Candidate algorithms

In previous inter-comparison exercises, undertaken as part of the OC-CCI programme, the empirical chlorophyll-a algorithms have consistently outperformed the results derived from semi-analytical models. This may have been due to the singular relationship used to convert IOPs into Chl-a estimates (following Bricaud et al, 1995), though an explanation of this difference is not required here. The number of available empirical algorithms has grown alongside our increased measurement and understanding of optical variability in the global oceans. There are now at least 65 empirical algorithms to derive chlorophyll-a from around 25 different satellite-based sensors. As this data record is bandshifted and bias corrected to give a 'single' sensor merged product, this number is vastly reduced for consideration but still leaves 8 readily available empirical algorithms for comparison with a MERIS-referenced merged sensor record. These algorithms are called NASA OC2, NASA OC3, NASA OC4,NASA OC5, OCI, OCI2, OC5CI and OCx, and are described below. All of these algorithms are available within SeaDAS and a summary of the algorithm as parameterised for MERIS is given.

The NASA Ocean Colour 2 (OC2) algorithm

The NASA OC2 chlorophyll algorithm (O'Reilly et al., 2019) uses a polynomial relationship between a log-transformed two band ratio (X) and the chlorophyll-a concentration. The band ratio is taken with a blue wavelength (closest to 490nm) and a green wavelength (usually the instrument band that falls within 545nm to 570nm). For MERIS the blue and green wavelengths are 490nm and 560nm respectively.

$$X = log_{10}\left(\frac{R_{rs}(\lambda_b)}{R_{rs}(\lambda_g)}\right) \tag{12}$$

The polynomial fit to the data is then of the form:

$$log_{10}(Chl) = a_0 + a_1X + a_2X^2 + a_3X^3 + a_4X^4 \tag{13}$$

where a_0 to a_4 are the fitted coefficients and for MERIS these are 0.2389,-1.9369,1.7627,-3.0777,-0.1054 respectively.

The NASA Ocean Colour 3 (OC3) algorithm

The NASA OC3 chlorophyll-a algorithm uses the same polynomial form as the OC2 but uses three wavebands for the calculation of *X* such that the blue wavelength is the maximum R_{rs} value over a defined range. For MERIS this is range includes the 443 and 490nm bands such that:

$$X = log_{10}\left(\frac{\max[R_{rs}(\lambda_{b1}), R_{rs}(\lambda_{b2})]}{R_{rs}(\lambda_g)}\right) \tag{14}$$

where λ_{b1} is 443nm and λ_{b2} is 490nm. The values of a_0 to a_4 for MERIS are then 0.2521, -2.2146, 1.5193, -0.7702, and -0.4291 respectively.

The NASA Ocean Colour 4 (OC4) algorithm

The NASA OC4 chlorophyll-a algorithm also uses the same polynomial form as the OC2 and OC3 but uses four wavebands for the calculation of *X* such that the blue wavelength is the maximum R_{rs} value over a defined range. For MERIS this is range includes the 443nm, 490nm and 510nm bands such that:

$$X = log_{10}\left(\frac{max[R_{rs}(\lambda_{b1}), R_{rs}(\lambda_{b2}), R_{rs}(\lambda_{b3})]}{R_{rs}(\lambda_g)}\right) \quad (15)$$

where λ_{b1} is 443nm, λ_{b2} is 490nm and λ_{b3} is 510nm. The values of a_0 to a_4 for MERIS are then 0.3255, -2.7677, 2,4409, -1.1288, and -0.4990 respectively.

The Ocean Colour 5 band (OC5) algorithm

In this context the OC5 algorithm does not refer to the NASA OC5 algorithm of O'Reilly et al. (2019) but instead to that of Gohin et al. (2002). This algorithm determines chlorophyll-a concentrations from triplet values of OC4 (as parameterised for MERIS) maximum band ratio, nLw(412) and nLw(560), using a Look Up Table (LUT), based on the relationships between measured Chl-a and satellite $R_{rs}(\lambda)$ from observations in the English Channel and Bay of Biscay (Gohin et al., 2002). The method has also been extended to the Mediterranean Sea and applied to MODIS-Aqua and MERIS (Gohin, 2011).

The Ocean Colour Index (OCI) algorithm

The Ocean Colour Index (OCI) chlorophyll algorithm was developed by Hu et al. (2012). This empirical algorithm was designed to improve the estimate of chlorophyll (C) in the global ocean at chlorophyll-a concentrations ≤0.25 mg m^{-3}.

$$CI = R_{rs,\lambda_2} - \left[R_{rs,\lambda_1} + \left(\frac{\lambda_2 - \lambda_1}{\lambda_3 - \lambda_1}\right)\left(R_{rs,\lambda_3} - R_{rs,\lambda_1}\right)\right], \quad (16)$$

where for MERIS λ_1, λ_2, and λ_3 are 443, 555 and 665. As MERIS does not contain a 555 band this is generated from the 560nm band using a relationship derived from NOMAD data in which:

$$R_{rs,555} = \begin{cases} 10^{v3\times\log_{10}(R_{rs,560})-v_4} \ if \ R_{rs,560} < 0.001148 & (17) \\ (v_1 \times R_{rs,560}) - v_2 \ if \ R_{rs,560} \geq 0.001148 & (18) \end{cases}$$

where v_1, v_2, v_3 and v_4 equal -0.103624, -0.000121, 1.023 and -0.103624 respectively. The CI chlorophyll-a estimate is then calculated as:

$$Chl_{CI} = 10^{aCI+b} \quad (19)$$

where *a is* 191.66 and *b* is -0.4909.

Following the approach of SeaDAS, the blending of the CI estimate of chlorophyll-a at low chlorophyll-a concentrations with the NASA OCx algorithm at higher concentrations occurs between chlorophyll-a concentrations of 0.15 and 0.2 mg m^{-3}, meaning that:

$$Chl_{OCI} = \begin{cases} Chl_{CI} & if\ Chl_{CI} < 0.15 \\ \left(Chl_{CI}\left(\frac{0.2 - Chl_{CI}}{0.05}\right)\right) + \left(Chl_{OC_x}\left(\frac{Chl_{CI} - 0.15}{0.05}\right)\right) & if\ 0.15 < Chl_{CI} < 0.2 \\ Chl_{OC_x} & if\ Chl_{CI} > 0.2 \end{cases} \quad (20)$$

The Ocean Colour Index 2 (OCI2) algorithm

The OCI2 algorithm is the updated version of the OCI algorithm as specified in Hu et al. 2019. This follows the same formulation as the OCI algorithm above but the coefficients *a* and *b* in equation 19 are set to 230.47 and -0.4287 such that:

$$Chl_{CI2} = 10^{230.47CI - 0.4287}, \quad (21)$$

and the blending thresholds are updated in equation 20 to give:

$$Chl_{OCI2} = \begin{cases} Chl_{CI2} & if\ Chl_{CI} < 0.25 \\ \left(Chl_{CI2}\left(\frac{0.4 - Chl_{CI2}}{0.15}\right)\right) + \left(Chl_{OC_x}\left(\frac{Chl_{CI2} - 0.25}{0.15}\right)\right) & if\ 0.25 < Chl_{CI} < 0.4 \\ Chl_{OC_x} & if\ Chl_{CI} > 0.4 \end{cases} \quad (22)$$

The Ocean Colour 5 band plus Colour Index (OC5CI) algorithm

The OC5CI algorithm is a blended algorithm which follows equation 19 but blends the CI Chlorophyll-a estimate with that of the OC5 algorithm described above and the blending window is set to 0.1 to 0.15 mg m^{-3}. This yields:

$$Chl_{OC5CI} = \begin{cases} Chl_{CI} & if\ Chl_{CI} < 0.1 \\ \left(Chl_{CI} \times \left(\frac{0.15 - Chl_{CI}}{0.05}\right)\right) + \left(Chl_{OC5} \times \left(\frac{Chl_{CI} - 0.1}{0.05}\right)\right) & if\ 0.1 < Chl_{CI} < 0.15 \\ Chl_{OC5} & if\ Chl_{CI} > 0.15 \end{cases} \quad (23)$$

The OCx band ratio algorithm

The NASA OCx algorithm (O'Reilly et al., 2000) as implemented in SeaDAS 7.5.3 implements the OC2, OC3 or OC4 algorithms depending upon which sensor is being processed. As we are processing data that is band shifted and bias corrected to appear as MERIS data, this algorithm is functionally identical to the OC4 algorithm in this case.

3.7.1.3 Match-up QC

As with the inter-comparison of atmospheric correction algorithms described above, a points scoring classification is used to objectively rank the performance of the algorithms. Before being permitted to contribute to the performance assessment, matchups between the output products and in situ data were passed through a number of quality checks as follows:

- Chlorophyll-a estimate is between 0.01 and 100.
- Water depth greater than 10m.
- Not exact duplicated values within 8km on day of measurement.
- Not derived from Argo float fluorescence data.
- Not acquired within the last year (to allow time for agency level QC).

Any matched chl-a pair which failed to meet all the above criteria was discarded.

3.7.1.4 Statistics and Scoring

It is important to bear in mind that some variables (such as chl-a) are log-normally distributed at the global scale. This means that for those variables the statistics and scoring should be performed on log-transformed values to allow the statistical relationships to hold true. To test the performance of the bio-optical algorithms the following univariate statistical tests were adopted that are commonly used in comparisons between modelled and in situ data (Doney et al., 2009; Friedrichs et al., 2009):

- Pearson correlation coefficient (r)
- bias (δ)
- centre-pattern (or unbiased) Root Mean Square Error (Δ)
- Slope (S) of a Type-2 regression
- Intercept (I) of a Type-2 regression
- Percentage of possible retrievals

3.7.1.4.1 Correlation Coefficient

As with the atmospheric round robin, the general approach is that for each metric the best model (and those that are statistically indistinguishable from it) would score 2 points, those close to deviating from the performance of the best would score 1 point, and those that were significantly different from the best would score 0 points. For each of the statistics this similarity is assessed slightly differently, as explained below.

The *r* test involved determining whether the *r*-value for each model was statistically lower than the model with an *r*-value closest to 1 (the best model). This was determined using the z-score. The z-score may be used to determine if two correlation coefficients are statistically different from one another (Cohen and Cohen, 1983). Knowing the *r*-value for two respective models (r_1 and r_2, for model 1 and 2 respectively) and knowing the number of samples used to determine the r-values (n_1 and n_2) one can determine the z-score using the Fisher's z transformation (Zar, 2014). Making use of the sample size employed to obtain each coefficient, these z-scores of each *r*-value (z_1 and z_2) can be used to compute the overall z-score (Cohen and Cohen, 1983), such that:

$$z_1 = 0.5 \log\left(\frac{1 + r_1}{1 - r_1}\right) \tag{24}$$

$$z_2 = 0.5 \log\left(\frac{1 + r_2}{1 - r_2}\right) \tag{25}$$

$$z_{score} = \frac{z_1 - z_2}{\left(\left[\frac{1}{n_1 - 3}\right]\left[\frac{1}{n_2 - 3}\right]\right)^{0.5}} \tag{26}$$

Having determined the z-score, this can be converted into a p-value assuming a normal distribution. For the model comparison, a two-tailed test is used and the score for each model is based upon the p-value as follows:

- 0 points if p-value for the model tested < 0.01 (i.e statistically different to the best model)
- 1 point if p-value for the model tested is ≥ 0.01 (i.e statistically similar to the best model)
- 2 points if p-value for the model tested is ≥ 0.05 (i.e statistically very similar to the best model). This is not cumulative with a point for being ≥ 0.01.

3.7.1.4.2 Bias

The closer the model bias (δ) is to the reference value of zero the better that model corresponds with the in situ data. However, a model could have a δ close to the reference value of zero, when compared with another model, but have a much larger 95 % confidence interval, implying lower confidence in the retrieved δ. Therefore, the following points classification was introduced for the bias:

- 0 points = the 95 % confidence interval of δ for a particular model is higher than the 1.5 times the smallest 95 % confidence interval of any model. In addition to this, the modulus of the bias ± its 95 % confidence interval did not overlap with zero.
- 1 point = either, the 95 % confidence interval of δ for a particular model less than 1.5 times the smallest model 95 % confidence interval, or the modulus of the bias ± its 95 % confidence interval overlaps with zero, but not both cases.
- 2 points = the 95 % confidence interval of δ for a particular model is less than 1.5 times the smallest model 95 % confidence interval and the bias ± its 95 % confidence interval overlaps with zero.
- For both bias and centre-pattern Root Mean Square Error statistics the 95% confidence interval is computed from the standard error of the mean and the t-distribution of the sample size such that:

$$Confidence\ Interval = t_{0.025,n-1}\frac{S_n}{\sqrt{n}}, \tag{27}$$

where S_n is the standard deviation of the error, *n* is the number of matchups and *t* is the two-tailed t-distribution.

3.7.1.4.3 Centre-pattern Root Mean Square Error

In addition to computing Δ for each model, it is possible to determine the confidence levels in Δ which provide an indication of how confident one is in the statistic. The confidence levels are computed from the standard error of the mean percentage and the t-distribution of the sample

size. Confidence levels provide a powerful way of highlighting differences and similarities between models. If the confidence intervals of two or more models overlap, then it can be assumed that the models have a statistically similar Δ at the given confidence interval. For each model, the 90 % and 95 % confidence intervals are computed for Δ. Points for each model are awarded on the following basis:

- 0 points = Δ for the model tested is statistically higher than the Δ for the best model (no overlap with a p-val of 0.01).
- 1 point = Δ for the model tested is statistically similar to the Δ for the best model (overlap with a p-val of 0.01).
- 2 points = Δ for the model tested is statistically very similar to the Δ for the best model (overlap with a p-val of 0.1).

3.7.1.4.4 Slope (S) and Intercept (I) of a Type-2 regression

In addition to computing the intercept (I) and the slope (S) from Type-2 regression, it is possible to compute the standard deviation on *I* and *S*. The closer the intercept (*I*) is to the reference value of zero and the closer the slope (S) is to the reference value of one the better the fit between variables. Similar to the Bias, a model could have an intercept closer to the reference value of zero and a slope closer to the reference value of one, when compared with another model, but have a much larger standard deviation on its retrieved parameters, implying lower confidence in the fit. Therefore, to account for both these possibilities the following points classification is implemented for the slope (*S*) parameter:

- 0 points = the standard deviation of the S parameter for a particular model is higher than 1.5 times the smallest standard deviation in S. In addition to this, the S parameter $\pm$ its standard deviation does not overlap with 1.
- 1 point = either, the standard deviation of the S parameter for a particular model is less than 1.5 times the smallest standard deviation or S $\pm$ its standard deviation overlaps with 1, but not both cases.
- 2 points = the standard deviation of the S parameter for a particular model is less than 1.5 times the smallest standard deviation and the S parameter $\pm$ its standard deviation overlaps with 1.

The following points classification was introduced for intercept (*I*) parameter:

- 0 points = the standard deviation of the I parameter for a particular model is higher than 1.5 times the smallest standard deviation in I. In addition to this, the I parameter $\pm$ its standard deviation does not overlap with that zero.
- 1 point = either the standard deviation of the I parameter for a particular model is less than 1.5 times the smallest standard deviation, or the I parameter $\pm$ its standard deviation overlaps zero, but not both cases.
- 2 points = the standard deviation of the I parameter for a particular model is less than 1.5 time the smallest standard deviation and the I parameter $\pm$ its standard deviation overlaps with zero.

3.7.1.4.5 Percentage of possible retrievals

To compare the percentage of possible retrievals (η) between models, highest percentage and standard deviation of retrievals for all models was used. The following points criteria were set-up:

- 0 points = η of a model lies further than 1 standard deviation below the maximum algorithm η.
- 1 point = η of a model lies within 1 standard deviation of the maximum η.
- 2 points = η of a model is equal to the maximum η.

3.6.1.5 Bootstrapping and multi-metric scoring

To rank the performance of each model with reference to a particular variable, all points were summed over the set of statistical tests used. The total score for each model was then normalised to the highest score for a single model. A score of one indicates the model scored the highest total number of points across all tests, with values less than 1 showing the points score of each model relative to the highest achieved. Figure 6 shows a flow-chart illustrating the methodology of the scoring system used to compare models.

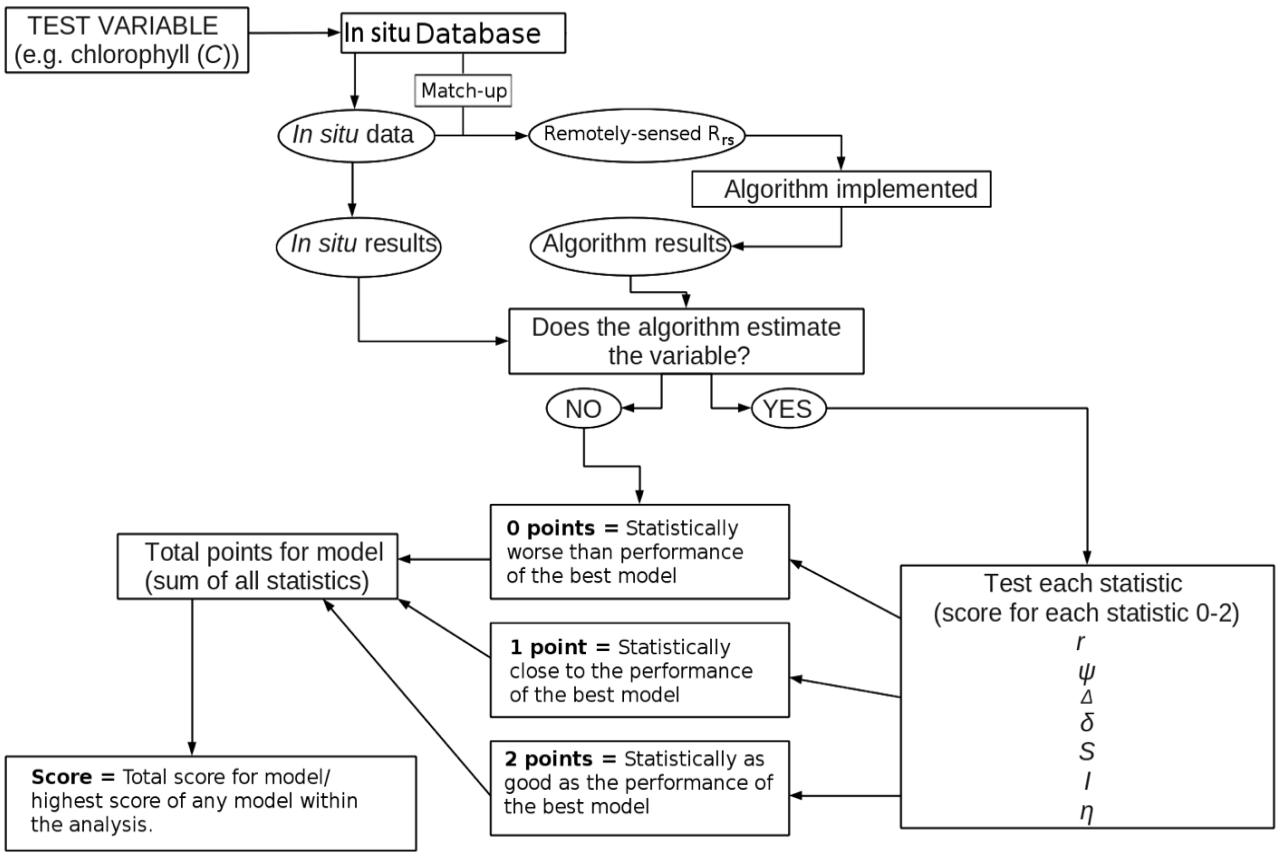

Figure 6: Flow chart of multi-metric scoring approach for Ocean Colour algorithm comparison

The stability of the scoring system, and the sensitivity of the scores, was tested using the method of bootstrapping (Efron, 1979; Efron and Tibshirani, 1993). This involves using sampling with replacement to randomly re-sample the in situ data to create 1000 new datasets, each the same size as the original dataset. The quantitative statistical methodology was then re-run for each new

dataset (Monte-Carlo approach) and from the resulting distribution of scores, a mean score for each model was computed. Additionally, a 2.5 % and a 97.5 % interval on the bootstrap distribution is taken and assumed to be the confidence limits on the mean score for each model, rather than standard deviations on the bootstrap distribution, to avoid misinterpretation of results should the bootstrap distribution not follow a normal distribution or be skewed, for instance due to the presence of outliers in the data.

3.7.1.6 Per-water-class assessment

The division of waters into optical types is an established concept in marine sciences. Morel and Prieur (1977) distinguished two water types - those where bulk optical properties are dominated by phytoplankton (Case-1) and those where bulk optical properties are uncoupled from phytoplankton (Case-2). This early division led to the development of 'Case- 1' and 'Case-2' algorithms which were tailored to produce the best results under a given set of assumptions about the optical nature of the waters in question. With the introduction of multidimensional clustering techniques applied to remote sensing data (Moore et al 2009, 2014), this classification of waters has become non-binary with >10 optical water types (OWT) identified in both open-ocean (Jackson et al., 2017) and inland-water (Spyrakos et al., 2018) environments.

The initial comparison and scoring of algorithms makes use of all the available in situ data. This in situ database has been collected in a variety of environments from open-ocean, clear waters to coastal environments with complex optical properties. In spite of a great deal of effort it is known that algorithms optimised to work in very clear waters are likely to perform worse in highly turbid waters, especially when compared to algorithms tailored for such environments. In order to assess the performance of the algorithms across a range of optical conditions the matched in situ and R_{rs} data are divided based on the dominant optical water class (for example, those defined in the OC-CCI processing chain). The waterclass set used in this case contained 14 optical waterclasses, defined based on their R_{rs} spectra normalised to the spectral integral. Each optical class subset was then run through the same scoring processing as the total dataset.

3.7.1.6.1 Chlorophyll-a concentration (mg m-3)

Chlorophyll-a in the C3S2-OC products has units of mg m^{-3} and is provided as daily products with a horizontal resolution of ~4 km/pixel. The chlorophyll-a values are calculated by blending algorithms based on the water-type memberships (as covered below) following the approach developed by OC-CCI.

A successful algorithm blending approach in the context of the C3S should combine algorithms seamlessly to produce the optimal resultant product without introducing boundary artefacts. To achieve this goal the OC-CCI project built upon the work of Moore et al. (2014). As part of the OC processing chain the R_{rs} spectra are assigned fuzzy memberships to a set of optical water classes detailed in Jackson et al. (2017). In the case of the v5.0 products this class set consisted of 15 optical water types defined for spectra normalised to the integral of the total visible spectrum.
An in-water algorithm round robin was performed to identify the optimal product algorithm for each water class in the set. The final chlorophyll-a product is then calculated by applying equation 20 to calculate the weighted product estimate per pixel:

$$P_w = \frac{\sum_{i=1}^{i=n} P_i W_i}{\sum_{i=1}^{i=n} W_i} \quad (28)$$

where P_w is the final weighted product value, P_i is the product estimated using the optimal algorithm for water class *i* and W_i is the pixel membership to water class *i*. The in-water round robin and bootstrapping exercise indicated that 4 of the 8 algorithms were optimal in at least one of the waterclasses.

Therefore, for the v6.0, this involved the application of each of the OCI, OCI2, OC2, and OCx algorithms[12]. An example of this is shown in Figure 7. Each algorithm utilises the same OC-CCI merged R_{rs} products above. Please note that while the chlorophyll values are provided in normal units, the uncertainty is based on log10 values due to the underlying natural distribution (see Figure 8 for an example).

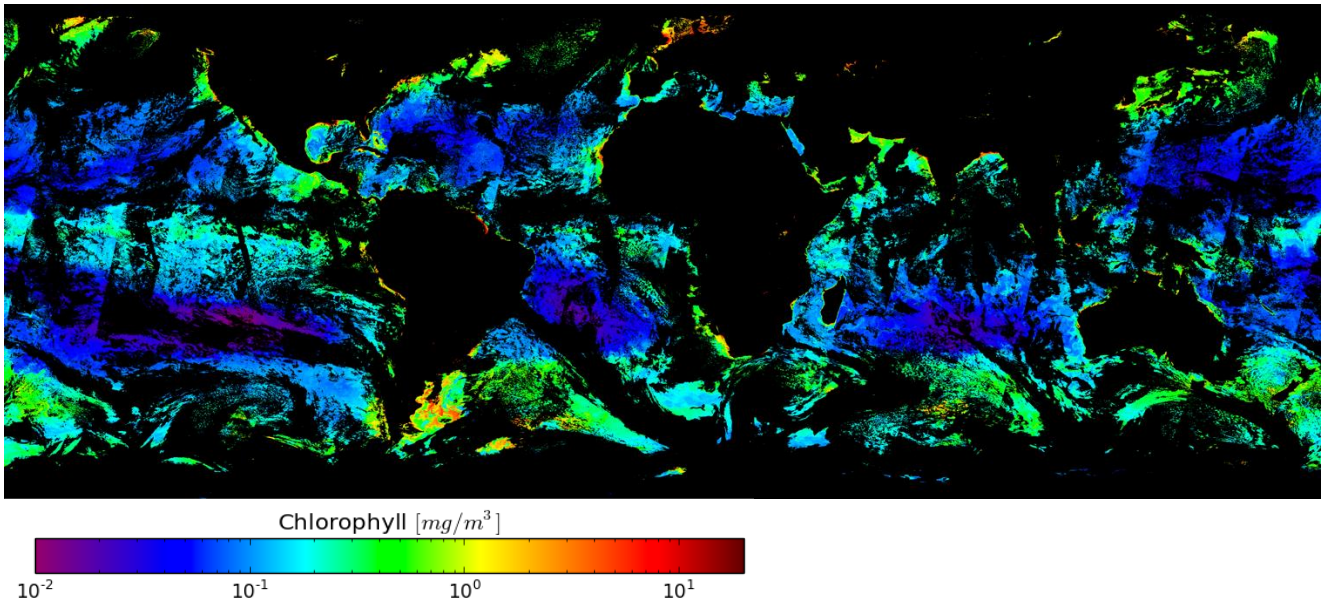

Figure 7: Global map of chlorophyll concentration (11/06/2017) resulting from blending of the OCI, OCI2, OC2, OC3, OCx and OC5 algorithms.

[12] Further details of these algorithms can be found in Section 3.7.1.2, and at https://oceancolor.gsfc.nasa.gov/atbd/chlor_a/ (accessed 8th September 2022)

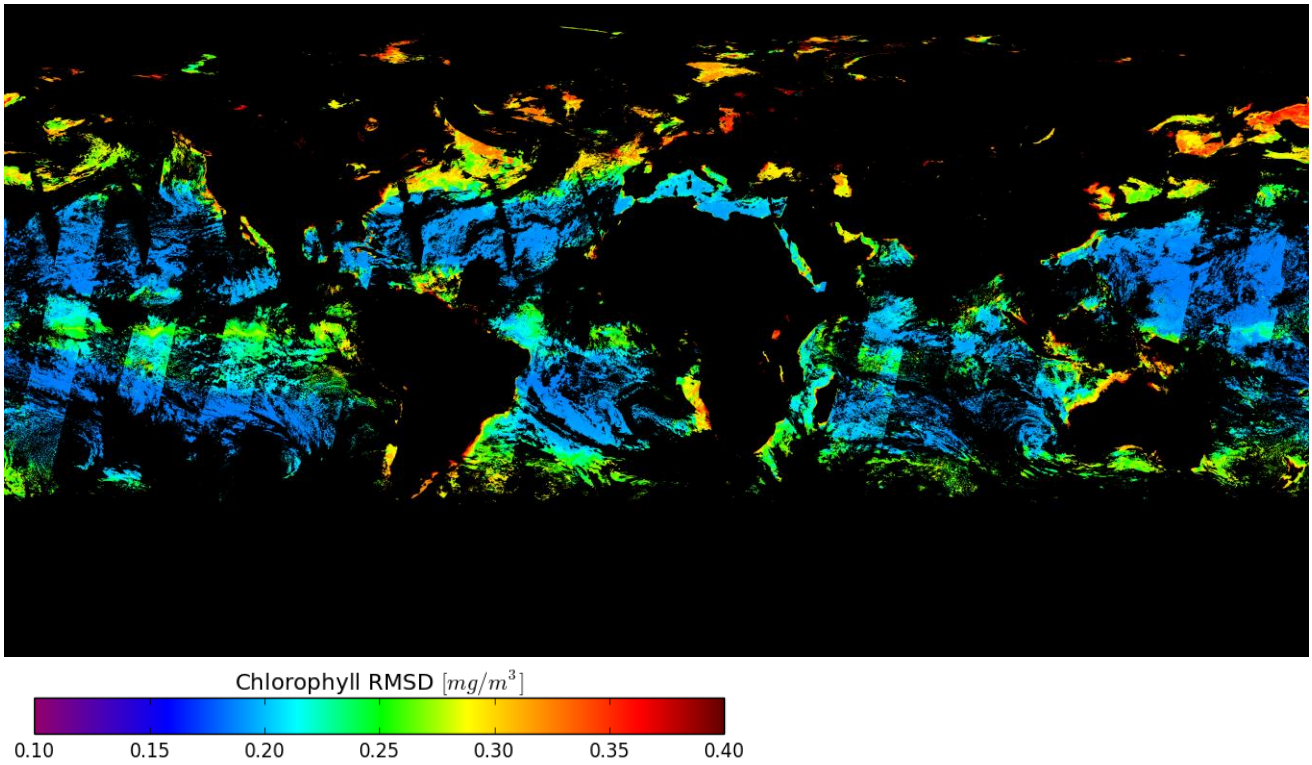

Figure 8: Global map of the root mean squared difference (RMSD) uncertainy in log10(Chlor_a). This highlights the lower uncertainty in the optically less complex gyres and higher uncertainty in the more complex coastal waters.

4. Output data

This section provides an overview of the data layers within and format of the output Version 6.0 Ocean colour data products (Chl-a, and R_{rs}). Further in-depth information on formats, metadata, file global and variable attributes, and conventions applied can be found in the Product User Guide and Specification document (C3S2_PUGS) listed in the related documents section.

4.1 General format description

The outputs of the C3S2 processing chain are level 3 mapped daily composites, generated from multiple sensors, with a spatial resolution of 4 km/pixel. The data are stored as CF-compliant NetCDF as has been mandated by the ESA CCI Data Standards Working Group. NetCDF version 4 is used because it allows for transparent internal compression of the data which would otherwise be approximately 15 times larger using NetCDF 3; hence, users need to ensure that their NetCDF libraries are at least version 4.0.0 (released 2008) or higher to be able to read these files. Familiarity with NetCDF terminology and general usage is assumed for this section. For the v6.0 data release, a typical NetCDF file containing the full set of products for a single day is approximately hundreds of megabytes.

4.2 Filename convention

The filename convention is:
ESACCI-OC-<Processing Level>-<Product String>-<Data Type>-<Additional Segregator>-<Indicative Date>[<Indicative Time>]-fv<File version>.nc

With the components above being:

- <Processing Level> for the OC-CCI processed products, 'L3S' will apply.
- <Product String> The Product String defines the source of the data set and depends on the processing level. For the OC-CCI processed products, 'MERGED' will apply
- <Data Type> This should contain a short term describing the main data type in the data set.
- <Additional Segregator> This is an optional part of the filename, containing information about spatial and temporal resolution, length of time period, processing center etc.
- <Indicative Date> The identifying date for this data set. Format is YYYY[MM[DD]].
- <Indicative Time> The identifying time for this data set in UTC. Format is [HH[MM[SS]]].

<File version> Dataset version for GHRSST compatibility; always the same as the CCI dataset version, e.g. “6.0” for the v6.0 data
An example filename is:
ESACCI-OC-L3S-CHLOR_A-MERGED-1D_DAILY_4km_GEO_PML_OCx-20031225-fv6.0.nc
With additional segregate elements being:

- GEO: Additional Segregator Element: Projection type (Geographic or Sinusoidal)
- PML: Additional Segregator Element: Processing Centre (fixed)
- OCx_QAA: Additional Segregator Element: Algorithm(s) (varies)

All files contain CF-compliant latitude and longitude (and time) dimensions, allowing each data cell to be specifically associated with a location. All latitudes and longitudes are given in WGS/84 datum.

4.3 File structure

This section provides an overview of all the dimensions and variables contained in the OC-CCI processed products. Since the data are provided on two different grids, there are two subsections describing the specific parts of these, while the majority of the variables are covered in one section below.

Specific elements of the sinusoidal products:

```
dimensions:
time = 1 ;
bin_index = 23761676
variables:
int crs ;
crs:grid_mapping_name = "1D binned sinusoidal" ;
crs:number_of_latitude_rows = 4320 ;
crs:total_number_of_bins = 23761676 ;
float Rrs_412(time, bin_index) ;
Rrs_412:grid_mapping = "crs" ;
float lon(bin_index) ;
lon:standard_name = "longitude" ;
lon:units = "degrees_east" ;
lon:axis = "X" ;
float lat(bin_index) ;
lat:standard_name = "latitude" ;
lat:units = "degrees_north" ;
lat:axis = "Y" ;
```

The sinusoidal projection has a primary dimension of bin_index, which is used by the data variables. Standard latitude and longitude variables exist and are indexed with the same dimension to provide world coordinates, via the standard “coordinates” attribute linking the data variables to the coordinate variables, per the CF convention. Time is included as a dimension, though is of length 1 for all products.

The ‘crs’ variable is a CF style grid mapping variable that describes and parameterises the sinusoidal projection and can be used as a definitive way to identify a sinusoidally projected variable. The contents of this variable are not yet accepted into the CF convention but follow the guidelines laid out for new projections.

Specific elements of the geographic products:

```
dimensions:
time = 1 ;
lat = 4320 ;
lon = 8640 ;
variables:
int crs ;
crs:grid_mapping_name = "latitude_longitude" ;
float chlor_a(time, lat, lon) ;
```

chlor_a:grid_mapping = "crs" ;

The geographic projection files are completely CF standard in terms of their projection descriptors. The ‘crs’ variable contains the standard element for a lat/long projection and all variables are dimensioned directly with time, latitude and longitude.

4.4 Flags

As the products are a composite both over time (one day) and of multiple sensors, it is not possible to preserve flags from the source datasets. This is in common with most level 3 compositing approaches. Instead, appropriate filtering was done as part of the binning stage, to exclude pixels flagged as “bad” (details in the [OC_CCI-SSD] document). This means that the flags used in the data filtering are not preserved into the output products, but they are listed earlier in this document.

References

Bricaud, A., Babin, M., Morel, A., and Claustre, H. (1995) Variability in the chlorophyll-specific absorption coefficients of natural phytoplankton: analysis and parameterization. *J. Geophys. Res.*, 100, 13321-13332.

Cohen, J., Cohen, P., (1983). Applied multiple regression/correlation analysis for the behavioural sciences. L. Erlbaum Associates.

Djavidnia, S., Mélin, F., and Hoepffner, N. (2010) Comparison of global ocean colour data records. *Ocean Sci.*, 61-76.

Doney, S. C., Lima, I. D., Moore, J. K., Lindsay, K., Behrenfeld, M. J., West- berry, T. K., Mahowald, N., M., G. D., Takahashi, T., (2009). Skill metrics for confronting global upper ocean ecosystem-biogeochemistry models against field and remote sensing data. Journal of Marine Systems 76, 95–112.

Efron, B., (1979). Bootstrap methods: another look at the jackknife. Annals of Statistics 7, 1–26.

Efron, B., Tibshirani, R. J., (1993). An Introduction to the Bootstrap. Chapman and Hall, New York.

Friedrichs, M. A. M., Carr, M.-E., Barber, R. T., Scardi, M., Antoine, D., Armstrong, R. A., Asanuma, I., Behrenfeld, M., Buitenhuis, E. T., Chai, F., Christian, J. R., Ciotti, A. M., Doney, S. C., Dowell, M., Dunne, J., Gentili, B., Gregg, W. W., Hoepffner, N., Ishizaka, J., Kameda, T., Lima, I., Marra, J., M´elin, F., Moore, J. K., Morel, A., O'Malley, R. T. O., O'Reilly, J. E., Saba, V. S., Schmeltz, M., Smyth, T. J., Tjiputraw, J., Waters, K., Westberry, T. K., Winguth, A. (2009). Assessing the uncertainties of model estimates of primary productivity in the tropical Pacific Ocean. Journal of Marine Systems 76 (1-2), 113–133.

Gohin, F., Druon, J.N. and Lampert, L. (2002) A five channel chlorophyll concentration algorithm applied to SeaWiFS data processed by SeaDAS in coastal waters. International journal of remote sensing, 23(8), 1639-1661, https://doi.org/10.1080/01431160110071879, 2002

Gohin, F., (2011). Annual cycles of chlorophyll-a, non-algal suspended particulate matter, and turbidity observed from space and in situ in coastal waters. Ocean Sci. 7, 705–732.

Hu, C., Lee, Z., Franz, B., (2012). Chlorophyll a algorithms for oligotrophic oceans: A novel approach based on three-band reflectance difference. Journal of Geophysical Research 117, C01011.

Hu, C., Feng, L., Lee, Z., Franz, B. A., Bailey, S. W., Werdell, P. J., & Proctor, C. W. (2019). Improving satellite global chlorophyll a data products through algorithm refinement and data recovery. Journal of Geophysical Research: Oceans, 124, 1524–1543. https://doi.org/10.1029/2019JC014941

IOCCG, 2017 Software for ocean colour algorithms, viewed 20/11/2021, <https://www.ioccg.org/groups/software.html>

Jackson, T., Sathyendranath, S., and Mélin F. (2017) An improved optical classification scheme for the Ocean Colour Essential Climate Variable and its applications, *Remote Sens. Environ.*, http://dx.doi.org/10.1016/j.rse.2017.03.036,.

Lee, Z.P., Carder, K.L., and Arnone, R.A. (2002) Deriving inherent optical properties from water color: a multiband quasi-analytical algorithm for optically deep waters. *Appl. Opt.*, 41, 5755-5772.

Lee, Z.P., Lubac, B, Werdell, J and Arnone, R. (2010) An Update of the Quasi-Analytical Algorithm (QAA_v5) http://www.ioccg.org/groups/Software_OCA/QAA_v5.pdf

Lee and Hu (2006) Zhong Ping Lee and Chuanmin Hu. Global distribution of Case-1 waters: An analysis from SeaWiFS measurements. Remote Sensing of Environment, 101:270-276, 2006.

Mélin, F., and Zibordi, G. (2007) An optically-based technique for producing merged spectra of water leaving radiances from ocean color. *Appl. Opt.*, 46, 3856-3869.

Mélin, F., Zibordi, G., and Berthon, J.-F. (2007) Assessment of satellite ocean color products at a coastal site. *Remote Sens. Environ.*, 110, 192-215.

Mélin, F., Vantrepotte, V. , Clerici, M., D'Alimonte, D., Zibordi, G. , Berthon, J.-F., and Canuti, E., (2011) Multi-sensor satellite time series of optical properties and chlorophyll a concentration in the Adriatic Sea," Prog. Oceanogr. **91**, 229–244.

Mélin, F. (2016) Impact of inter-mission differences and drifts on chlorophyll-*a* trend estimates, International Journal of Remote Sensing, 37:10, 2233-2251, DOI: 10.1080/01431161.2016.1168949,.

Moore, T. S., Campbell, J. W., & Dowell, M. D. (2009) A class-based approach to characterizing and mapping the uncertainty of the MODIS ocean chlorophyll product. *Remote Sens. Environ.*, 113, 2424-2430, doi:10.1016/j.rse.2009.07.016.

Moore, T., Dowell, M. D., Bradt, S., and Verdu, A. R. (2014) An optical water type framework for selecting and blending retrievals from bio-optical algorithms in lakes and coastal waters. *Remote Sens. Environ.*, 143:97–111.

Morel, A. and Prieur, L. (1977). Analysis of variations in ocean color. *Limnol. Oceanogr.,* 22: 709-722.

Morel, A., and Gentili, B. (1991) Diffuse reflectance of oceanic waters: its dependence on Sun angle as influenced by the molecular scattering contribution. *Appl. Opt.*, 30, 4427-4438.

Morel, A., and B. Gentili (1996) Diffuse reflectance of oceanic waters. III. Implication of bidirectionality for the remote-sensing problem. *Appl. Opt.*, 35, 4850-4862.

Morel, A., Antoine, D., and Gentili, B. (2002) Bidirectional reflectance of oceanic waters: accounting for Raman emission and varying particle scattering phase function. *Appl. Opt.*, 41, 6289-6306.

O'Reilly, J. E., Maritorena, S., O'brien, M. C., Siegel, D. A., Toole, D., Menzies, D., Smith, R. C., Mueller, J. L., Mitchell, B. G., Kahru, M., & Chavez, F. P. (2000). SeaWiFS Postlaunch calibration and validation analyses, Part 3. In S. B. Hooker & E. R. Firestone (Eds.), NASA Tech. Memo. 2000–206892 (Vol. 11, 49 pp.). Greenbelt, MD: NASA Goddard Space Flight Center.

O'Reilly, J.E., Werdell, P. Jeremy (2019) Chlorophyll algorithms for ocean color sensors - OC4, OC5 & OC6, Remote Sensing of Environment, Volume 229, Pages 32-47, ISSN 0034-4257, doi: 10.1016/j.rse.2019.04.021.

Park, Y.-J., and Ruddick, R. (2005) Model of remote sensing reflectance including bidirectional effects for case 1 and case 2 waters. *Appl. Opt.*, 44, 1236-1249.

Platt, T., Hoepffner, N., Stuary, V., Brown, C. (2008) Why Ocean Colour? The Societal Benefits of Ocean Colour Technology. IOCCG Report Number 7, 2008. Available at: https://ioccg.org/wp-content/uploads/2015/10/ioccg-report-07.pdf [last accessed 10/10/2022]

Pope, R.M, and Fry, E.S. (1997) Absorption spectrum (380-700nm) of pure water. II. Integrating cavity measurements. *Appl. Opt.*, 36, 8710-8723.

Spyrakos, E., O'Donnell, R., Hunter, P.D., Miller, C., Scott, M., Simis, S.G.H., Neil, C., Barbosa, C.C.F., Binding, C.E., Bradt, S., Bresciani, M., Dall'Olmo, G., Giardino, C., Gitelson, A.A., Kutser, T., Li, L., Matsushita, B., Martinez-Vicente, V., Matthews, M.W., Ogashawara, I., Ruiz-Verdú, A., Schalles, J.F., Tebbs, E., Zhang, Y. and Tyler, A.N. (2018), Optical types of inland and coastal waters. Limnol. Oceanogr., 63: 846-870.

Steinmetz, F., Deschamps, P-Y., and Ramon D., (2011) Atmospheric correction in presence of sun glint: application to MERIS, Opt. Express 19, 9783-9800

Valente, A., Sathyendranath, S., Brotas, V., Groom, S., Grant, M., Jackson, T., Chuprin, A., Taberner, M., Airs, R., Antoine, D., Arnone, R., Balch, W. M., Barker, K., Barlow, R., Bélanger, S., Berthon, J.-F., Beşiktepe, Ş., Borsheim, Y., Bracher, A., Brando, V., Brewin, R. J. W., Canuti, E., Chavez, F. P., Cianca, A., Claustre, H., Clementson, L., Crout, R., Ferreira, A., Freeman, S., Frouin, R., García-Soto, C., Gibb, S. W., Goericke, R., Gould, R., Guillocheau, N., Hooker, S. B., Hu, C., Kahru, M., Kampel, M., Klein, H., Kratzer, S., Kudela, R., Ledesma, J., Lohrenz, S., Loisel, H., Mannino, A., Martinez-Vicente, V., Matrai, P., McKee, D., Mitchell, B. G., Moisan, T., Montes, E., Muller-Karger, F., Neeley, A., Novak, M., O'Dowd, L., Ondrusek, M., Platt, T., Poulton, A. J., Repecaud, M., Röttgers, R., Schroeder, T., Smyth, T., Smythe-Wright, D., Sosik, H. M., Thomas, C., Thomas, R., Tilstone, G., Tracana, A., Twardowski, M., Vellucci, V., Voss, K., Werdell, J., Wernand, M., Wojtasiewicz, B., Wright, S., and Zibordi, G. (2022) A compilation of global bio-optical in situ data for ocean-colour satellite applications – version three, Earth Syst. Sci. Data Discuss. [preprint], https://doi.org/10.5194/essd-2022-159, in review, 2022.

Zar, J.H., (2014). Spearman Rank Correlation: Overview. Wiley StatsRef: Statistics Reference Online. doi:10.1002/9781118445112.stat05964

Zhang, X., Hu, L., and He, M.-X. (2009) Scattering by pure seawater: Effect of salinity. *Opt. Exp.*, 17, 5698-5710.

Zibordi, G., Berthon, J.-F. Mélin, F., D'Alimonte, D. and S. Kaitala, (2009) Validation of satellite ocean color primary products at optically complex coastal sites: northern Adriatic Sea, northern Baltic Proper, Gulf of Finland, Remote Sens. Environ. 113, 2574–2591.

Zibordi, G., Mélin, F., Berthon, J.-F. (2012a) Trends in the bias of primary satellite ocean color products at a coastal site. *IEEE Geosci. Remote Sens. Lett.*, 9, 1056-1060, 10.1109/LGRS.2012.2189753.

Zibordi, G., Mélin, F., Berthon, J.-F. (2012b) Intra-annual variations of biases in remote sensing primary ocean color products at a coastal site. *Remote Sens. Environ.*, 124, 627-636.

Copernicus Climate Change Service

ECMWF - Shinfield Park, Reading RG2 9AX, UK

Contact: https://support.ecmwf.int/

climate.copernicus.eu copernicus.eu ecmwf.int